Developmental Biology 330 (2009) 406–426

Contents lists available at ScienceDirect

Developmental Biology

journal homepage: www.elsevier.com/developmentalbiology

Anatomy of zebrafish cerebellum and screen for mutations affecting its development

Young-Ki Bae [a,b,1], Shuichi Kani [a,1], Takashi Shimizu [a,1], Koji Tanabe [a], Hideaki Nojima [a], Yukiko Kimura [c], Shin-ichi Higashijima [c], Masahiko Hibi [a,d,*]

[a] Laboratory for Vertebrate Axis Formation, RIKEN Center for Developmental Biology, Kobe, Hyogo, Japan
[b] Division of Basic and Applied Sciences, Research Institute, National Cancer Center, Republic of Korea
[c] National Institutes of Natural Sciences, Okazaki Institute for Integrative Bioscience, Aichi, Japan
[d] Bioscience and Biotechnology Center, Nagoya University, Nagoya, Japan

ARTICLE INFO

Article history:
Received for publication 14 November 2008
Revised 6 April 2009
Accepted 7 April 2009
Available online 14 April 2009

Keywords:
Cerebellum
Hindbrain
Purkinje cells
Granule cells
Eurydendroid cells
Climbing fibers
Mossy fibers
Parallel fibers
Neural circuits
Mutant screening
Zebrafish

ABSTRACT

The cerebellum is important for the integration of sensory perception and motor control, but its structure has mostly been studied in mammals. Here, we describe the cell types and neural tracts of the adult zebrafish cerebellum using molecular markers and transgenic lines. Cerebellar neurons are categorized to two major groups: GABAergic and glutamatergic neurons. The Purkinje cells, which are GABAergic neurons, express parvalbumin7, carbonic anhydrase 8, and aldolase C like (zebrin II). The glutamatergic neurons are *vglut1*$^{+}$ granule cells and *vglut2*^{high} cells, which receive Purkinje cell inputs; some *vglut2*^{high} cells are eurydendroid cells, which are equivalent to the mammalian deep cerebellar nuclei. We found *olig2*$^{+}$ neurons in the adult cerebellum and ascertained that at least some of them are eurydendroid cells. We identified markers for climbing and mossy afferent fibers, efferent fibers, and parallel fibers from granule cells. Furthermore, we found that the cerebellum-like structures in the optic tectum and antero-dorsal hindbrain show similar Parvalbumin7 and Vglut1 expression profiles as the cerebellum. The differentiation of GABAergic and glutamatergic neurons begins 3 days post-fertilization (dpf), and layers are first detectable 5 dpf. Using anti-Parvalbumin7 and Vglut1 antibodies to label Purkinje cells and granule cell axons, respectively, we screened for mutations affecting cerebellar neuronal development and the formation of neural tracts. Our data provide a platform for future studies of zebrafish cerebellar development.

Introduction

The cerebellum functions in the control of smooth and skillful movements. It is also implicated in a variety of cognitive and emotional functions (Ito, 2008; Rodriguez et al., 2005). The cerebellum integrates sensory and predictive inputs, which include proprioception and information associated with motor commands, to elicit precise motor control and higher cognitive/emotional functions (Bell, 2002; Bell et al., 2008; Ito, 2002a,b, 2006). These complex tasks rely on the well-organized structure of the cerebellum and neural circuits.

There are several different types of neurons in the bony fish (teleost) cerebellum (Fig. 1A). They can be categorized into two groups based on their functions as excitatory or inhibitory neurons (Altman and Bayer, 1997; Butler and Hodos, 1996). The excitatory neurons use glutamate as their major neurotransmitter (glutamatergic neurons). They include granule cells, eurydendroid cells, and unipolar brush cells (UBC). The inhibitory neurons utilize gamma-aminobutyric acid (GABA) and/or glycine (GABAergic/glycinergic neurons), and include Purkinje cells and interneurons such as the Golgi and stellate cells. The cerebellar neurons receive excitatory input from neurons in the pre-cerebellar nuclei, outside the cerebellum, and these afferent axons are classified into two groups, mossy fibers and climbing fibers (Fig. 1A). The climbing fibers originate from neurons in the inferior olive nucleus (IO) in the posterior hindbrain and innervate Purkinje cell dendrites. The mossy fibers originate from neurons in the pre-cerebellar nuclei (excluding IO), and they synapse onto the same granule cell dendrites that are in contact with the axons of Golgi cells to form the cerebellar glomeruli.

Information from the mossy fibers is conveyed to the dendrites of Purkinje cells by the axons of granule cells, called parallel fibers, and the information from the climbing and mossy fibers is integrated by the Purkinje cells. The neural activity of the climbing fibers suppresses synaptic transmission from the axons of granule cells by a mechanism called long-term depression (LTD), which is important for motor learning (Ito, 2002a,b, 2006). Purkinje cells send their axons to either adjacent Purkinje cells or eurydendroid cells (Alonso et al., 1992; Meek et al., 1992), while the eurydendroid cells send efferent axons to other regions of the brain (Ikenaga et al., 2005; Murakami and Morita, 1987). These neurons and neural fibers are arranged in a three-layer structure in the cerebellum, from superficial to deep: the molecular layer (ML), Purkinje cell layer (PCL or ganglionic layer), and granule

* Corresponding author. Laboratory for Vertebrate Axis Formation, RIKEN Center for Developmental Biology, Kobe, Hyogo, Japan. Fax: +81 78 3063136.
E-mail address: hibi@cdb.riken.jp (M. Hibi).
[1] These authors contributed equally to this work.

0012-1606/$ – see front matter © 2009 Elsevier Inc. All rights reserved.
doi:10.1016/j.ydbio.2009.04.013

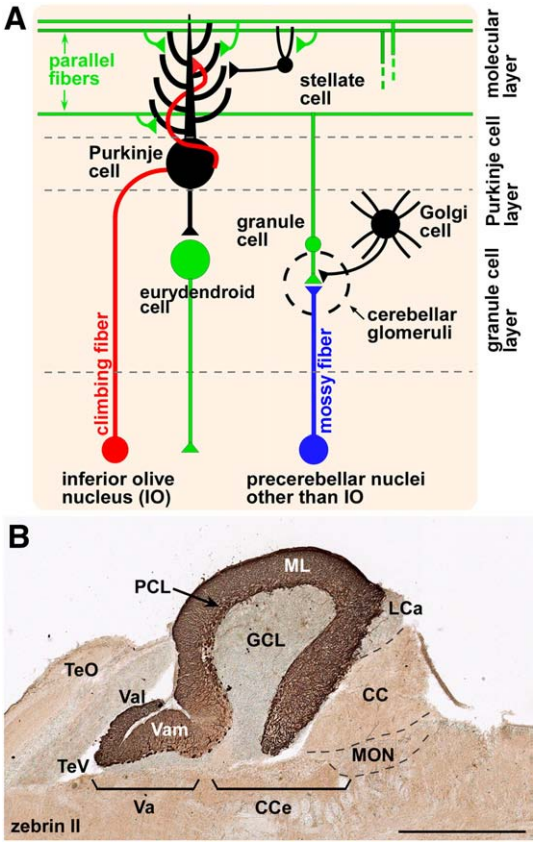

Fig. 1. Cerebellar neurons and circuits. (A) Schematic presentation of zebrafish cerebellar neurons and circuits. (B) Zebrin II immunohistochemistry of a sagittal section of adult cerebellum. DAB staining. Anterior is to the left. CC, crista cerebellaris; CCe, corpus cerebelli; GCL, granule cell layer; LCa, lobus caudalis cerebelli; ML, molecular layer; MON, medial octavolateralis nucleus; PCL, Purkinje cell layer; TeO, tectum opticum; TeV, tectal ventricle; Va, valvula cerebelli; Vam, medial division of valvula cerebelli; Val, lateral division of the valvula cerebelli. Scale bars: 500 μm (B).

cell layer (GCL). In the ML, the dendrites of Purkinje cells receive inputs from the climbing fibers and granule cell axons, and from stellate interneurons. There are synaptic interactions among mossy fibers, granule cells, and interneurons in the cerebellar glomeruli of the GCL.

The teleost cerebellum is composed of three major parts: the valvula cerebelli (Va), the corpus cerebelli (CCe), and the vestibulolateral lobe which consists of the eminentia granularis (EG) and the lobus caudalis cerebelli (LCa) (Miyamura and Nakayasu, 2001; Wullimann et al., 1996) (Fig. 1B). The Va and CCe display the same three-layer structure, whereas the vestibulolateral lobe (EG and LCa) only contains the GCL. In addition, the crista cerebellaris (CC) and medial octavolateralis nucleus (MON) in the dorsal hindbrain of teleosts are proposed to function as part of the cerebellum ("cerebellum-like structures"), because parallel fibers of granule cells are located in the EG and run along the CC, contacting the dendrites of the crest cells whose cell bodies are in the MON [EG-CC-MON circuitry] (Bell et al., 2008; Mikami et al., 2004; Volkmann et al., 2008). Similarly, type I neurons, which are also known as pyriform cells, in the optic tectum (Meek and Schellart, 1978) extend their dendrites superficially to receive inputs from the parallel fibers from the torus longitudinalis (TL) in the stratum marginale (SM) [TL-SM-Type I neuron circuitry] (Bell et al., 2008; Mikami et al., 2004; Volkmann et al., 2008).

There are a few differences between the teleost and mammalian cerebellum. The mammalian cerebellum lacks eurydendroid cells and, in its place, the deep cerebellar nuclei (DCN) play a functionally homologous role, as they receive the axons of Purkinje cells and send efferent axons. The DCN are located ventrally, far from the Purkinje cells, whereas eurydendroid cells are located in the vicinity of the PCL. Although the mammalian DCN and teleost eurydendroid cells are both projection neurons that send axons outside the cerebellum, it is not known if they use the same molecular machineries for their function and development. All of the granule cells lie underneath the PCL in the mammalian cerebellum. In the teleost cerebellum, the granule cells in the Va and CCe are underneath the PCL, whereas the granule cells in the EG and LCa are located superficially and send their axons to the CC (Folgueira et al., 2006; Montgomery, 1981; Puzdrowski, 1989; Volkmann et al., 2008). Although these granule cells may function differently from those in the GCL of the Va and CCe, it is not known if they use the same genes for their growth and differentiation or if they use the same molecular machineries for the formation of parallel fibers.

The zebrafish cerebellum forms in the anterior hindbrain during the embryonic and larval periods. The glutamatergic neurons are derived from progenitors located at the upper rhombic lip (URL) and express the proneural gene *atoh1* (*Math1* in mice) (Alder et al., 1996; Ben-Arie et al., 1997). *atoh1*-expressing URL progenitors generate the granule cells and the DCN in mice (Machold and Fishell, 2005; Wang et al., 2005; Wilson and Wingate, 2006; Wingate, 2005). The glutamatergic neurons in the zebrafish cerebellum show a similar developmental process (Koster and Fraser, 2001; Volkmann et al., 2008), although it hasn't been thoroughly characterized in detail. In the mouse, the GABAergic neurons are derived from progenitors in the ventricular zone (VZ) that express the proneural gene *ptf1a* (Hoshino, 2006; Hoshino et al., 2005). *ptf1a* is also expressed in the zebrafish cerebellum (Lin et al., 2004; Zecchin et al., 2004), but its precise expression domain and role have not been reported. In addition, neurons expressing the proneural gene *olig2* are located in the vicinity of the PCL in the zebrafish cerebellum and extend long neurites, like the eurydendroid cells (McFarland et al., 2008). The origin and functions of these *olig2*$^{+}$ neurons, however, remain to be elucidated.

Genetic and molecular studies, including mutant screening in zebrafish, have revealed genes that are involved in the initial process of cerebellum development, that are related to patterning of the hindbrain and formation of the midbrain–hindbrain boundary (Brand et al., 1996; Schier et al., 1996). These genes include *pax2a (no isthmus)* (Brand et al., 1996), *islet3* (Kikuchi et al., 1997), *fgf8 (acerebellar)* (Reifers et al., 1998), *pou2 (spiel ohne grenzen)* (Belting et al., 2001), and *wnts* (Buckles et al., 2004). Little is known, however, about what genes control the specification and neurite formation of individual cerebellar neurons in zebrafish. This is partly due to a lack of anatomical information about and molecular markers for the zebrafish cerebellum.

Here, we investigated the anatomy of the zebrafish cerebellum using molecular markers and transgenic lines. We describe the individual cell types and neural tracts within and connected to the cerebellum. We found that the differentiation of the cerebellar neurons begins at 3 days post fertilization (dpf), and we detected a simple layered structure as early as 5 dpf. Using antibodies that recognize the Purkinje and granule cell axons, we screened zebrafish cerebellar mutants and isolated lines that displayed defects in the development of cerebellar neurons and their neurites. These data provide anatomical information about the zebrafish cerebellum for comparative and developmental analyses, and are a source for genetic studies of cerebellar development.

Materials and methods

Zebrafish wild-type, transgenic lines and staging

Wild-type zebrafish (*Danio rerio*) with the Oregon AB genetic background were used. Transgenic lines *Tg(olig2:EGFP)vu12* (Shin

et al., 2003), *Tg(ptf1a:eGFP)jh1* (Pisharath et al., 2007), and *Tg (pou4f1-hsp70l:EGFP)rw0110b* (Aizawa et al., 2005) were previously described. The *Tg(vglut2a:EGFP)* line was constructed using the BAC DKEY-145P24 by a previously described method (Kimura et al., 2006). The details for generating this line will be described elsewhere. Zebrafish were reared as described (Westerfield, 1995). For immunohistochemistry and whole-mount in situ hybridization, embryos and larvae were treated with 0.005% phenylthiourea from 12 h post-fertilization to prevent pigmentation. Developmental stages were determined according to the Zebrafish Information Network (ZFIN: http://zfin.org/). Adult fish in this report characterize fish 90 days or older; juvenile fish are between 30 and 89 days old; larvae are between 3 and 29 days old.

In situ hybridization

The detection of *vglut1*, *vglut2a*, and *vglut2b* was described previously (Higashijima et al., 2004a,b). The cDNAs of *gad1*, *gad2* (Higashijima et al., 2004a,b), *pvalb7* (NM_205574), *lhx1a (lim1)* (Toyama et al., 1995), *aldocl* (NM_001029952), *ca8* (NM_001017571), *barhl1.1*, *barhl1.2* (Colombo et al., 2006), *eomesa* (Bruce et al., 2003), *calbidin2* (Rohrschneider et al., 2007), *fabp7a (blbp)* (Adolf et al., 2006), *glasta* (*slc1a3a*, NM_212640), *glastb* (*slc1a3b*, XM_679025), *glastc* (*slc1a3c*, NM_001109703), *mbp* (Brosamle and Halpern, 2002), *olig2* (Park et al., 2002), and *alcam* (NM_131000) were obtained by reverse-transcriptase-PCR from zebrafish embryos, larvae, and adult brains and were used to generate riboprobes. The detailed information about these probes is available on request.

For the in situ hybridization of sections, the brains were removed from adult zebrafish and fixed overnight at 4 °C in 4% paraformaldehyde (PFA) in phosphate-buffered saline (PBS). The specimens were immersed in 30% sucrose solution overnight at 4 °C, frozen in OCT compound (Sakura Finetechnical), and sectioned at 12–14 μm with a cryostat. The frozen sections were washed three times with Tris-buffered saline (TBS) for 10 min, treated with 0.2 M HCl for 10 min, and washed three times with TBS. They were subsequently treated with 0.1 M Tris–HCl (pH 8.0) containing acetic anhydride for 10 min and washed three times with TBS. They were incubated in hybridization buffer (50% formamide, 5× standard saline citrate [SSC], 50 μg/ml heparin, 0.1% Tween20, 5 mg/ml torula RNA) for more than 1 h and hybridized with a digoxigenin-UTP- or FITC-UTP-labeled riboprobe at 65 °C overnight. The specimens were rinsed with TBS and washed with 50% formamide 2× SSC at 65 °C, 50% formamide 1× SSC, and 20% formamide 0.5× SSC for 30 min each. They were then rinsed with TBS, incubated with blocking solution (1× Roche blocking reagent, 5% heat-inactivated fetal bovine serum, TBS) for 30 min, and incubated with 1/2000 diluted alkaline phosphatase (AP)-conjugated anti-digoxigenin, 1/500 diluted horseradish peroxidase (HRP)-conjugated anti-digoxigenin or anti-FITC antibodies (Roche) in the blocking buffer at room temperature (RT) for 30–60 min. After three washes with TBST (TBS containing 0.1% Tween20), the signals were examined. Whole-mount in situ hybridization was performed principally as described previously (Jowett and Yan, 1996).

For the single-color observation of section and whole-mount in situ hybridization, NBT/BCIP (Roche) was used as the substrate for AP. For two-color fluorescence in situ hybridization, tyramide signal amplification (TSA) kits with Alexa Fluor 488 tryamide and Alexa Fluor 555 tyramide (Molecular Probes, Invitrogen) were used to visualize the fluorescent signals. The first HRP reaction in the TSA procedure was terminated by incubating the sample in 0.1 M Glycine–HCl (pH 2.2) at RT for 1 h and washing three times with TBST, followed by staining with the second HRP-conjugated antibody and TSA reagent (Horikawa et al., 2006). The NBT/BCIP signals were acquired using an AxioPlan-2 microscope and AxioCam CCD camera (Zeiss). The fluorescence images were obtained as described below (under "Immunohistochemistry").

Generation of monoclonal and polyclonal antibodies

To raise monoclonal antibodies against parvalbumin7 (Pvalb7, NP_991137), carbonic anhydrase 8 (Ca8, NP_001017571), and Fabp7a (Blbp: NP_571680), glutathione S-transferase (GST) fusion proteins containing amino acids (aa) 1–109 of Pvalb7, aa 1–147 of Ca8, and aa 1–132 of Fabp7a (Blbp) were generated in *E. coli* BL21DE3. The GST fusion proteins were purified by Glutathione Sepharose 4B (GE Healthcare) and used for immunization. Balb/c mice were immunized four or five times with about 50 μg of the proteins. Spleen cells of the immunized mice were fused with the mouse myeloma line Ag8.563, and hybridomas were obtained by conventional HAT selection. Supernatants of growth-positive cells were subjected to enzyme-linked immunosorbent assays (ELISAs) to identify hybridoma clones producing specific antibodies. Polyclonal antibodies against Vglut1, Vglut2a, and Gad1 were generated by immunizing rabbits with the synthetic peptides CVGTNSYLYGGEGERELT, CDGVEEGGYGYRQGGNYS, and SAGDMDPNTANLRQPATC (the underlined C was added to link the peptides covalently with keyhole limpet hemocyanin), respectively. The anti-Vglut1 and anti-Gad1 antibodies were purified using peptide affinity columns that were generated by a SulfoLink Kit (Pierce).

Immunohistochemistry

For immunostaining, anti-zebrin II (1/200, hybridoma supernatant) (Lannoo et al., 1991a,b), anti-Pvalb7 (1/1000, mouse ascites), anti-Ca8 (1/100, mouse hybridoma supernatant), anti-Fabp7a/Blbp (1/1000, mouse ascites), anti-Sox10 (1/500) (Park et al., 2005, 2007), anti-Mbp (1/50) (Lyons et al., 2005), anti-BrdU (1/1000, BD Bioscience), zn5 (1/200) (Trevarrow et al., 1990), anti-HuC/D (1/500, mouse, Molecular Probes, Invitrogen), anti-Vglut1 (1/1000, purified antibody), anti-Vglut2a (1/2000, rabbit serum), anti-Gad1 (1/2000, purified antibody), anti-GAD1/2 (1/100, mouse ascites, Biomol), anti-calretinin (1/1000, rabbit, Swant) and anti-GFP (1/1000 mouse or rabbit, Nacalai) antibodies were used.

For whole-mount immunostaining, zebrafish larvae were fixed at 4 °C in 4% PFA in PBST (PBS, 0.1% Triton X-100) for 3 h. The fixed larvae were washed with PBST, and incubated in acetone at −30 °C for 15 min. Larvae or cryosections were washed once with PBST and twice with PBS-DT (PBS, 1% BSA, 1% DMSO, 1% Triton X-100), and incubated in 5% goat serum (Vector), PBS-DT at RT for 1 h. The samples were incubated with the primary antibody solution at 4 °C overnight. After four washes with PBST, the samples were incubated with secondary antibodies (1/1000 dilution, Alexa Fluor 488 and/or Alexa Fluor 555 goat anti-mouse and/or goat anti-rabbit IgG (H + L), Molecular Probes, Invitrogen). For two-color staining with two mouse monoclonal antibodies (Fig. 2N), a Zenon antibody labeling kit (Molecular Probes, Invitrogen) was used. The Vectastain Elite ABC kit (Vector) was also used for immunostaining with the HRP substrate diaminobenzidine (DAB, Figs. 1B, 3J, 3K, 5I). When the samples were stained with a riboprobe and antibody, in situ hybridization (NBT/BCIP or TSA staining) was performed first, followed by immunostaining (DAB or fluorescence).

The fluorescence images and DAB signals were obtained with a LSM5 Pascal laser scanning inverted microscope and AxioPlan-2 microscope, respectively. The fluorescence images were constructed from *Z*-stack sections by a 3D projection program associated with the microscope. Figures were constructed using Adobe Photoshop. Alexa Fluor 488 and 555 signals were colored green and magenta, respectively, for the figures.

Morpholino oligonucleotides

The antisense morpholino oligonucleotides (MOs) were generated by Gene Tools (LLC, Corvallis, OR, USA). The sequences of *vglut1*MO,

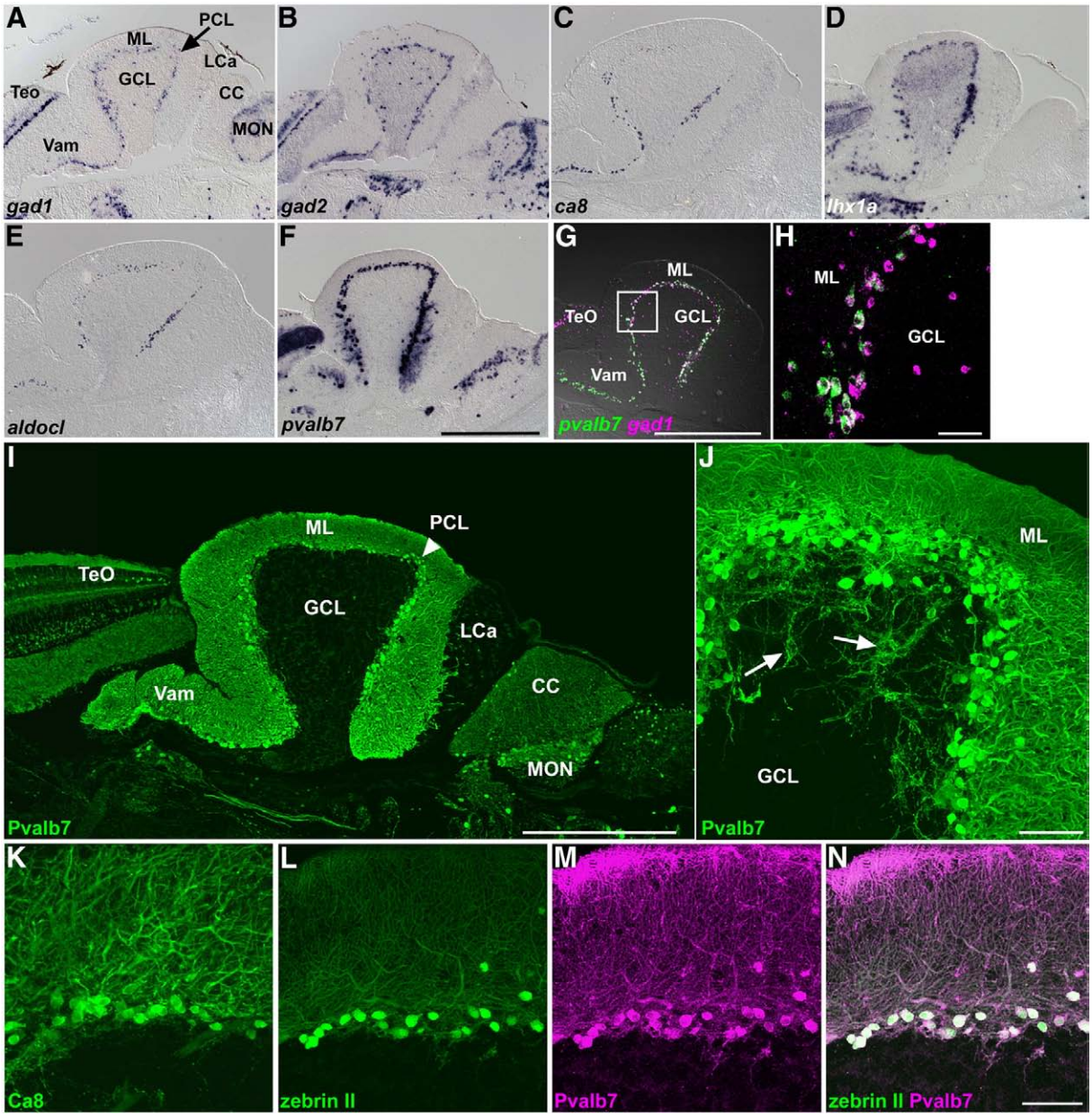

Fig. 2. GABAergic neurons. (A–F) Expression of *gad1* (A), *gad2* (B), *carbonic anhydrase 8* (*ca8*, C), *lhx1a* (*lim1*, D), *aldolase c-like* (*aldocl*, E), and *parvalbumin7* (*pvalb7*, F) in the adult cerebellum. In situ hybridization of sagittal sections. Anterior is to the left. (G, H) Comparison of *pvalb7* (green) and *gad1* (magenta) expression. (H) High-magnification view of the box in G. Note that all the *pvalb7*$^+$ cells are *gad1*$^+$ (white), but there are *gad1*$^+$ *pvalb7*$^-$ cells (magenta) in the GCL and ML. (I, J) Fluorescence immunohistochemistry of adult cerebellum with an anti-parvalbumin7 antibody (Pvalb7). Low (I) and high (J) magnification views. The position of the PCL is indicated by an arrowhead (I). Axons of Purkinje cells are indicated by arrows (J). Pvalb7$^+$ axons reach and surround Pvalb7$^-$ cells (indicated by arrows), which correspond to eurydendroid cells (J). (K–N) Anti-carbonic anhydrase 8 (Ca8, K), zebrin II (L) and anti-parvalbumin7 (Pvalb7, M) antibody staining. Zebrin II (green) and Pvalb7 (magenta) staining completely overlap (N). The abbreviations are described in Fig. 1. Scale bars: 500 μm (F, G, I) and 50 μm (H, J, N).

*vglut2a*MO, and *gad1*MO were 5′-CAGCACTGATACTGACCACTATGAC-3′, 5′-GCTCCCTCGGAGTCTCCATGTCCAA-3′, and 5′-AAGGTGCAGAAGAC-GCCATCAGTCC-3′, respectively. The MOs were dissolved in and diluted with water and injected into the yolk of one-cell-stage embryos.

BrdU incorporation

Adult zebrafish were kept in 1% BrdU (5′-bromo-2′deoxyuridine, Wako) solution for 1 h in the dark. The brains were removed and fixed in 4% PFA in PBS. The cryosections were treated with 2 N HCl for 30 min at room temperature, washed twice with PBS, 0.1% Tween20, neutralized twice with 0.1 M $Na_2B_4O_7$, and washed twice with PBS, 0.1% Tween20. Immunostaining was carried out as described above.

Retrograde labeling of eurydendroid cell axons and cerebellovestibular tracts

The retrograde labeling was carried out essentially as described previously (Ikenaga et al., 2005). Adult zebrafish were anesthetized in 100 mg/l ethyl m-aminobenzoate methanesulfonate (Nacalai). The cranium was removed by forceps and the optic tectum and CCe were exposed. 5-10 μl of 10% solution of dextran, tetramethylrhodamine and biotin (10,000 MW, lysine fixable, Molecular Probes, Invitrogen) was injected into the region underneath the optic tectum (the pretectal region, for detection of eurydendroid cell axons) or into the antero-lateral hindbrain (vestibular region including descending octaval nucleus-DON, for detection of cerebellovestibular tracts)

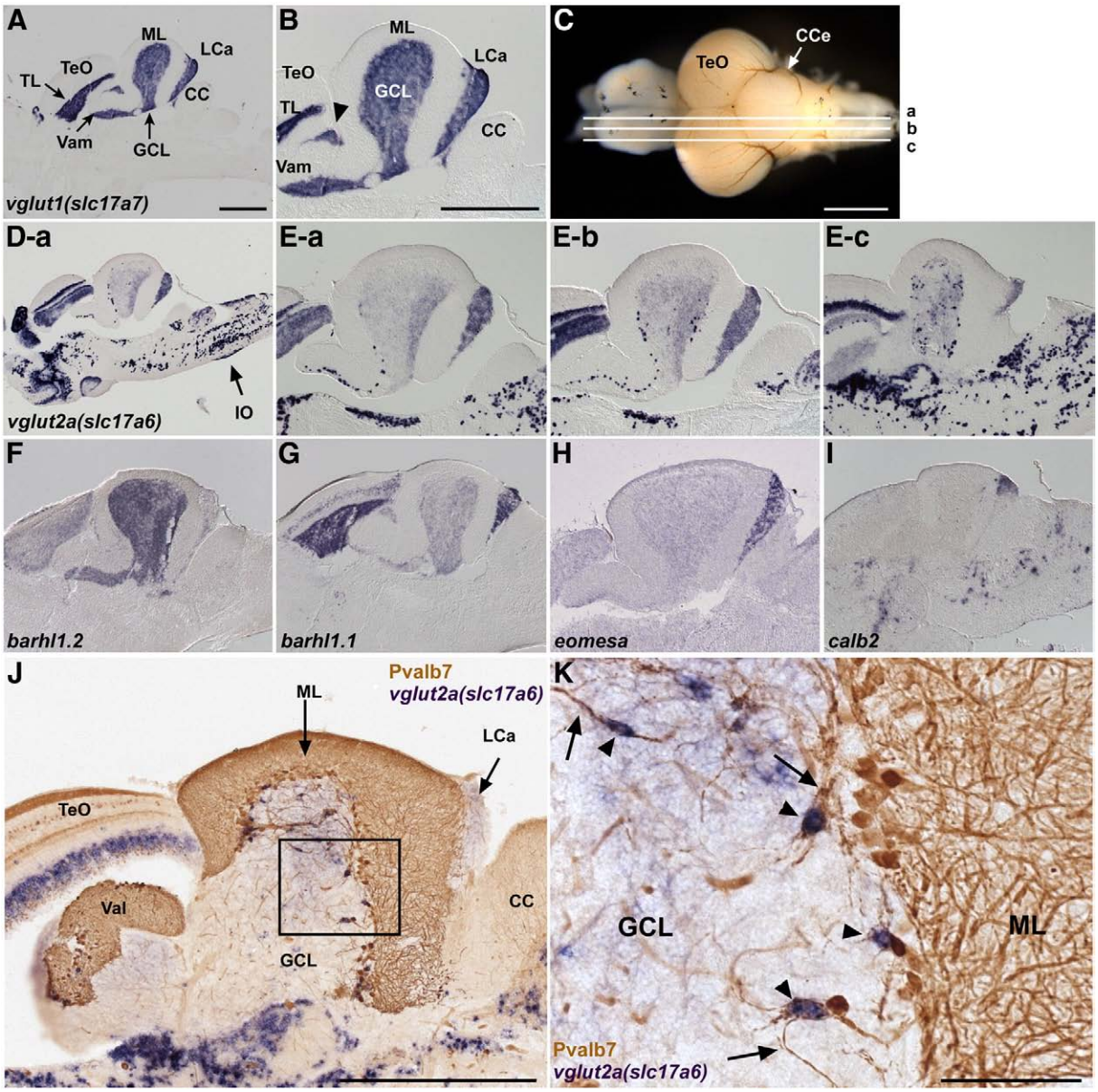

Fig. 3. Glutamatergic neurons. (A, B) Expression of *vglut1 (slc17a7)* in the adult cerebellum. In situ hybridization of a sagittal section. Low (A) and high (B) magnification views. Anterior is to the left. *vglut1* expression is detected in the torus longitudinalis (TL) of the TeO and the GCL of the Va, CCe, and LCa. The *vglut1*$^{+}$ region between TeO and GCL (indicated by arrowhead) belongs to the GCL (Suppl. Fig. 1). (C, D, E) Expression of *vglut2a (slc17a6)*. Sagittal sections at the levels (a medial, b mediolateral, c lateral.) shown in (C) were stained with a *vglut2a (slc17a6)* riboprobe. Low (D-a) and high (E-a, E-b, E-c) magnification views. *vglut2a*^{high} cells were scarcely observed in the medial region (D-a), but many were detected in more lateral regions (E-b, E-c). Expression of *vglut2a (slc17a6)* in the inferior olive nucleus is marked by an arrow (D-a). (F–I) Differential expression of *barhl1.2* (F), *barhl1.1* (G), *eomesodermin a* (*eomesa*, H), and *calbindin2* (*calb2*, I). (J, K) *vglut2a*^{high} eurydendroid cells. Co-staining with a *vglut2a* riboprobe (purple, NBT/BCIP staining) and anti-Pvalb7 antibody (brown, DAB staining). (K) High-magnification view of the box in J. Note that *vglut2a*^{high} cells (arrowheads) receive inputs from the Pvalb7^{+} axons of Purkinje cells (arrows). The abbreviations are described in Fig. 1. Scale bars: 500 μm (A, B, C, J) and 100 μm (K). The magnification of D and E–I are the same as in A and B, respectively.

with a Hamilton syringe driven by a micromanipulator (Narishige). The exposed brain regions were re-covered with the removed cranium. After 48 h of survival, the brain was removed and fixed in 4% PFA in PBST. The cryosections were stained with antibodies and 1 μg/ml of avidin, NeutrAvidin, Rhodamine Red-X conjugate (Molecular Probes, Invitrogen).

Immunoblotting

The brain (olfactory bulb, forebrain, midbrain, and hindbrain) was removed from an adult fish and homogenized with a hand pestle (Toyobo) in 500 μl of lysis buffer (50 mM Tris–HCl pH 7.4, 150 mM NaCl, 5 mM EDTA, 1% NP40) on ice. The lysate was cleared by centrifugation, and 1 μl of the lysate per lane was separated on a 5–20% SDS polyacrylamide gel (SuperSep, Wako) and transferred to a PVDF membrane (Immobilon, Millipore). The protein was detected with rabbit anti-sera and an HRP-conjugated goat anti-rabbit IgG (H + L) antibody (Zymed). The signals were visualized using a chemiluminescence system (Western Lightning; Perkin Elmer Life Science).

Mutant screening

Zebrafish mutants were generated as described previously (Driever et al., 1996; Haffter et al., 1996). The F1 generation was made by crossing ethyl nitrosourea (ENU)-treated AB male fish and non-treated female fish. The F2 family was established by crossing F1 male and female fish. F3 larvae obtained by crossing pairs of F2

animals were reared until 5 dpf. After fixation, the larvae were stained with an anti-Pvalb7 antibody (mouse monoclonal, to screen 256 mutated genomes), or anti-Pvalb7 and anti-Vglut1 (rabbit polyclonal) antibodies (to screen 520 mutated genomes), the signals of which were visualized with fluorescent secondary antibodies. The stained embryos were observed with a Leica MZ16F dissection fluorescence microscope. Families of larvae that showed an abnormal expression of Pvalb7 and/or Vglut1 were subjected to further analyses.

Results

Molecular markers for GABAergic neurons

To determine the individual cell types in the adult zebrafish cerebellum, we first examined the expression of orthologs of genes known to be expressed in GABAergic and glutamatergic neurons of the mammalian cerebellum (Figs. 2, 3, and Table 1). In teleost fish, as in mammals, GABAergic neurons express glutamic acid decarboxylase Gad1 (Gad67) and Gad2 (Gad65) (Castro et al., 2006; Higashijima et al., 2004a; Martin et al., 1998; Martyniuk et al., 2007; Meek et al., 2008), which convert glutamate into GABA in a single-step reaction. In the adult zebrafish cerebellum, *gad1* is expressed strongly in the Purkinje cells (Figs. 2A, G, H), consistent with a previous report (Martyniuk et al., 2007). *gad1* is also expressed weakly in non-Purkinje GABAergic neurons in the ML and GCL (Figs. 2A, G, H, and Table 1), which are presumably stellate and Golgi cells. *gad2* is expressed in both Purkinje cells and other GABAergic neurons in the ML and GCL, but its expression is more prominent in the non-Purkinje GABAergic neurons (Fig. 2B).

We found that *carbonic anhydrase 8* (*ca8*) and *lhx1a* (*lim1*) are expressed in Purkinje cells (Figs. 2C, D), as reported for the mammalian cerebellum (Hirota et al., 2003; Kato, 1990; Nogradi et al., 1997; Schuller et al., 2006). *lhx1a* was also detected weakly in a small number of cells in the GCL, which may include undifferentiated Purkinje cells, and also found expressed outside the cerebellum (Fig. 2D). The anti-zebrin II antibody recognizes the parasagittal compartments of Purkinje cells in mammals and most, if not all, of the Purkinje cells in the teleost cerebellum (Gravel and Hawkes, 1990; Lannoo et al., 1991a,b; Meek et al., 1992) (Figs. 1B, 2L). The zebrin II antigen is encoded by the *aldolase C* gene (Ahn et al., 1994). In zebrafish, there are two *aldolase C* genes, *aldoc* (*aldolase c, fructose-bisphosphate*) and *aldocl* (*aldolase c, fructose-bisphosphate-like*; Zebrafish Information Network, ZFIN:http://zfin.org/). We found that *aldocl* is expressed specifically in Purkinje cells (Fig. 2E). Parvalbumin, a Ca^{++}-binding protein, is expressed in Purkinje cells and other GABAergic interneurons in the chick, mammalian, and teleost cerebellum (Celio, 1990; Celio and Heizmann, 1981; Crespo et al., 1999; Jande et al., 1981; Porteros et al., 1998). There are at least nine *parvalbumin* genes in zebrafish (ZFIN). We found that *parvalbumin7* (*pvalb7*) is expressed in the Purkinje and crest cells, but not in the other GABAergic neurons in the zebrafish cerebellum (Fig. 2F).

To analyze the structure of the Purkinje cells, we raised monoclonal antibodies against parvalbumin7 (Pvalb7) and carbonic anhydrase 8 (Ca8). Both the anti-Pvalb7 and anti-Ca8 antibodies recognized the dendrites, soma, and axons of the Purkinje cells, which are located in the ML, PCL, and GCL, respectively, just as the anti-zebrin II and M1 antibodies do (Jaszai et al., 2003; Miyamura and Nakayasu, 2001) (Figs. 2I, J, K). Pvalb7 and zebrin II staining completely overlapped in the cerebellum (Figs. 2L, M, N). In the mammalian cerebellum, parvalbumin and Ca8 are expressed in all the Purkinje cells, but zebrin II is only detected in a particular Purkinje cell compartment (Brochu et al., 1990; Celio, 1990; Gravel and Hawkes, 1990; Hirota et al., 2003; Kato, 1990; Nogradi et al., 1997). In the zebrafish cerebellum, the Pvalb7, Ca8, zebrin II (Aldocl), and M1 antigen are all expressed in all of the Purkinje cells (Miyamura and Nakayasu, 2001). Although Pvalb7 is also expressed in the crest cells of the MON, Ca8 and zebrin II (Aldocl) were not (Figs. 1B, 2C, E, F, I).

Characterization of glutamatergic neurons

We next examined the expression of glutamatergic neuronal markers in the adult cerebellum (Fig. 3). Vesicular glutamate transporters *Vglut1* and *Vglut2* are expressed differentially in granule cells during mammalian cerebellar development (Hisano et al., 2002; Miyazaki et al., 2003). We found that *vglut1* (*slc17a7*: solute carrier family 17, member 7) is expressed only in the granule cells; whereas *vglut2a (slc17a6)* and *vgult2b (slc17a6l)* are only weakly expressed in the granule cells (the expression is relatively strong in the granule cells in the LCa), but are highly expressed in a subset of glutamatergic neurons near the PCL in the GCL (Figs. 3A, B, D and E; data not shown for *vglut2b*; the expression of *vglut2a* and *vglut2b* is essentially identical). The *vglut2*^{high} neurons (expressing *vglut2a*/*b* at high levels) are more abundant in the lateral region than in the medial region, indicating a laterally biased localization of *vglut2*^{high} neurons (Fig. 3E). Although *Vglut1* is also expressed in mossy fiber neurons in mammals (Hisano et al., 2002), in the zebrafish *vglut1*$^{+}$ cells were detected in the torus longitudinalis (TL) and habenula nuclei, but not in the pretectal regions, ventral midbrain, or hindbrain, where most of the mossy fiber neurons are localized (Fig. 3A). In contrast, *vglut2a* and *vglut2b* are expressed broadly in the pretectal regions, midbrain and hindbrain, including the IO in the ventro-medial region of the hindbrain (Fig. 3D, data not shown for *vglut2b*), indicating that most, if not all, of the pre-cerebellar glutamatergic neurons are *vglut2*$^{+}$.

Table 1
Cell-specific markers of zebrafish cerebellar neurons.

	Cells expressing the marker	Protein localization
GABAergic neurons		
gad1	Purkinje cells, Golgi, and stellate cells (PC>others*[1]), crest cells	T
gad2	Purkinje cells, Golgi, and stellate cells (PC<others*[2]), crest cells	
parvalbumin7	Purkinje cells and crest cells	S, A, D
aldolase c-like (aldocl)	Purkinje cells	S, A, D
carbonic anhydrase 8 (ca8)	Purkinje cells	S, A, D
lhx1a (lim1)	Purkinje cells	
Glutamatergic neurons		
vglut1(slc17a7)	Granule cells (CCe, EG, and LCa)	T
vglu2a(slc17a6)	Eurydendroid cells, granule cells*[3], mossy fiber neurons	T
vglut2b(slc17a6l)	Eurydendroid cells, granule cells*[3], mossy fiber neurons	T
zic1	Granule cells	
reelin	Granule cells	
pax6	Granule cells	
barhl1.1	Granule cells (Va/CCe/EG<LCa) *[4]	
barhl1.2	Granule cells (Va/CCe/EG>LCa) *[5]	
eomesa (tbr2)	Granule cells (Va/CCe/EG<LCa) *[4]	
calbindin2	Granule cells (LCa)	
Anti-calretinin ab	Eurydendroid cells in ML*[6]	
olig2	Eurydendroid cells in ML and GCL*[7]	
Glia		
blbp(fabp7)	Bergmann glia	C
glastb(slc1a3b)	Bergmann glia	
myelin basic protein (mbp)	Oligodendrocyte	

The expression of genetic markers was determined by in situ hybridization of sagittal sections of adult brain. The localization of proteins was determined using antibodies established in this study, as described. T, axon terminal; S, soma; A, axons; D, dendrites; C, cytosol. *[1,2]Expression was stronger*[1] or weaker*[2] in Purkinje cells compared to other GABAergic neurons in the cerebellum. *[3]Weak expression of *vglut2a* and *vglut2b* was detected in granule cells. *[4,5]Expression was stronger*[5] or weaker*[4] in the valvula cerebelli (Va), the corpus cerebelli (CCe), and the eminentia granularis (EG) than in the lobus caudalis cerebelli (LCa). *[6]Detection of some eurydendroid cells by anti-calretinin antibody is reported (Castro et al., 2006). *[7]Expression of *olig2* in some eurydendroid cells at larval stages is reported (McFarland et al., 2008).

The expression patterns of *reelin*, *pax6*, and *zic1* are homogenous in the GCL of the adult cerebellum (Table 1), as in the larval and juvenile stages of zebrafish and in the mammalian cerebellum (Aruga et al., 1994; Costagli et al., 2002; Foucher et al., 2006; Jaszai et al., 2003; Mueller and Wullimann, 2005), suggesting that all granule cells are similar as regards their expression of these markers. However, we found that some markers are differentially expressed by the granule cells located in the Va, CCe, EG, and LCa. The homeobox gene *barh-like 1.2* (*barhl1.2*) is expressed more highly in the granule cells of the Va, CCe and EG than in those of the LCa (Fig. 3F, Suppl. Fig. 2, and Table 1), whereas the T-box gene *eomesodermin homolog a* (*eomesa*, also known as *tbr2*) and *barhl1.1* are expressed more highly in the LCa than in the Va, CCe and EG, and the Ca^{++}-binding protein *calbindin2* is expressed only in the LCa (Figs. 3G, H, I, Suppl. Fig. 2 and Table 1).

Eurydendroid cells, which receive inputs from Purkinje cell axons, are localized near the PCL in the teleost cerebellum (Folgueira et al., 2006; Ikenaga et al., 2005; Porteros et al., 1998). The *vglut2*^{high} neurons were detected in the vicinity of the *pvalb7*$^{+}$ Purkinje cells, suggesting that some of the *vglut2*^{high} neurons are eurydendroid cells. To address this possibility, we stained sections of the adult cerebellum with a *vglut2a* riboprobe and/or an anti-Pvalb7 antibody. Most of the *vglut2*^{high} neurons are surrounded by Pvalb7^{+} Purkinje cell axons in the GCL, but do not express Pvalb7 (Figs. 2J, 3J, and 3K), indicating that they are eurydendroid cells.

Characterization of the glia

Although the Bergmann glia are relatively well characterized in mammals, little is known about them in the teleost cerebellum. Since BLBP (brain lipid-binding protein, or Fabp7: fatty acid binding protein 7) is expressed in Bergmann glial cells (Arnold et al., 1994; Feng and Heintz, 1995; Rousselot et al., 1997), we examined the expression of *blbp (fabp7a)* (Adolf et al., 2006; Rohrschneider et al., 2007) in the adult zebrafish cerebellum (Figs. 4A, B, and C). We found that *blbp (fabp7a)* is expressed strongly in the medial region near the PCL, but it is relatively weak in the lateral regions of Va and, anterior and posterior CCe (Figs. 4A, B, and C). We raised a monoclonal antibody against Blbp (Fabp7) that could recognize its expression in the hindbrain at the embryonic stage (data not shown). In the adult cerebellum, the anti-Blbp (Fabp7) antibody recognized cells with a palisade morphology, which is a characteristic feature of Bergmann glia (Castejon, 1990; de Blas, 1984; Meek and Nieuwenhuys, 1991), and the signal is strong in the ML of the Va and the antero-medial CCe (Figs. 4D, E, and F), suggesting that the Bergmann glia are

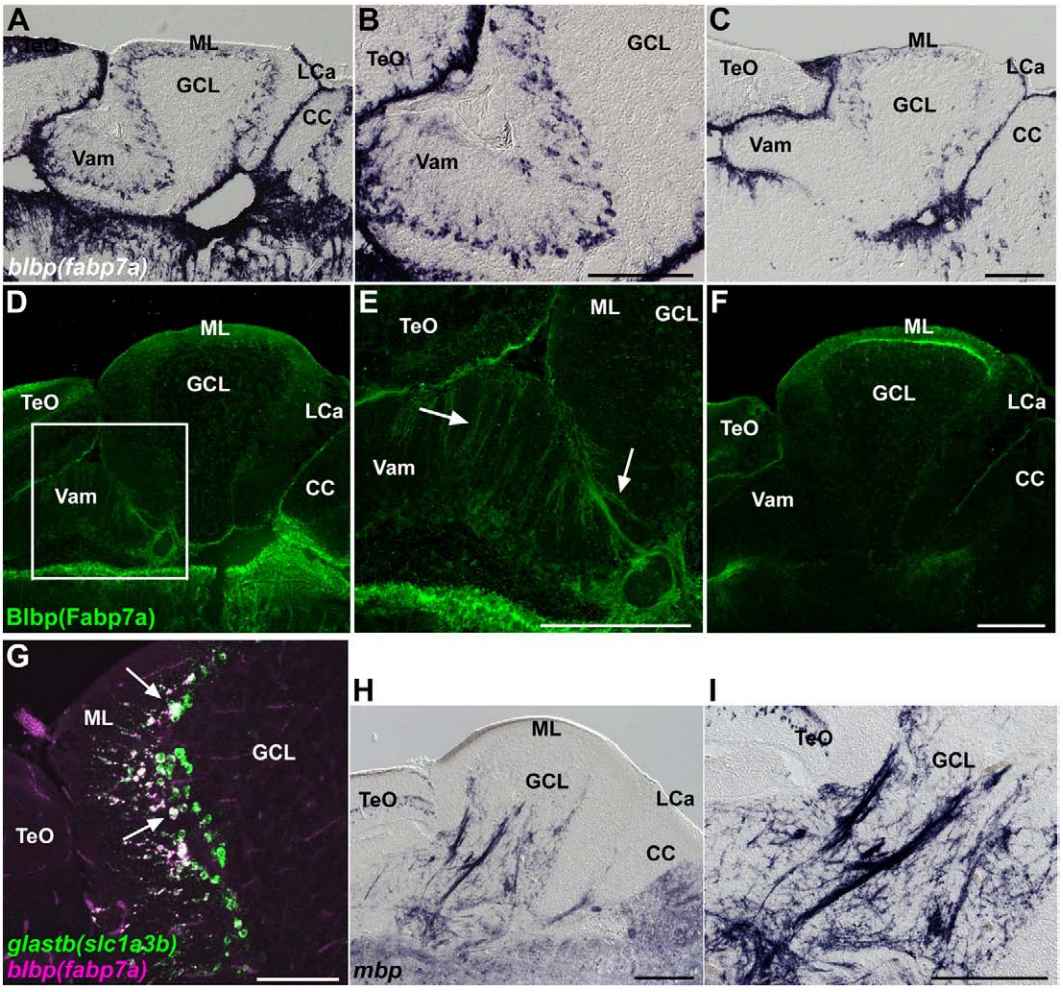

Fig. 4. Bergmann glia, and oligodendrocytes, and *olig2*$^{+}$ cells. (A–C) Expression of *blbp (fabp7a)*. Sagittal sections of the medial (A, B) and lateral (C) regions of the adult cerebellum. Low (A, C) and high (B) magnification views. (D–F) Immunostaining of Blbp (Fabp7a). Sagittal sections of the medial (D, E) and lateral (F) regions of the cerebellum. Low (D, F) and high (E) magnification views. The palisade structure of the Bergmann glial cells is indicated by arrows. Note that *blbp* is expressed strongly in the medial region, but it is relatively weak in the lateral regions of Va and, anterior and posterior CCe. Blbp was detected in the Va and dorsal CCe (both medial and lateral regions). (G) Expression of *glastb* (*slc1a3b)* and *blbp (fabp7a*) in adult cerebellum. Note that most of *fabp7a*-expressing Bergmann glial cells express *glastb* (indicated by white arrows). (H, I) Expression of *myelin basic protein* (*mbp*). Low (H) and high (I) magnification views. The abbreviations are described in Fig. 1. Scale bars: 200 μm (C, E, F, H, I) and 100 μm (G).

distributed unevenly among the regions of the adult cerebellum. Although GFAP (glial fibrillary acidic protein) is a known marker for Bergmann glia in mammals (de Blas, 1984; de Blas and Cherwinski, 1985), *gfap* expression was not detected in the Bergmann glia in the zebrafish adult cerebellum (data not shown). In the mature cerebellum of mammals, Bergmann glia processes ensheath synapses on Purkinje cell dendritic spines; Bergmann glia express the astrocyte-specific glutamate transporter GLAST and function as glutamate scavengers (Bellamy, 2006). We found three zebrafish *glast* (solute carrier family 1, member 3 [*slc1a3*]) genes from the database: *glasta* (*slc1a3a*), *glastb* (*slc1a3b*) and *glastc* (*slc1a3c*). Expression of *glastb* (*slc1a3b*) was detected in Blbp$^+$ Bergmann glial cells (Fig. 4G), consistent with the role of Bergmann glia as glutamate scavengers.

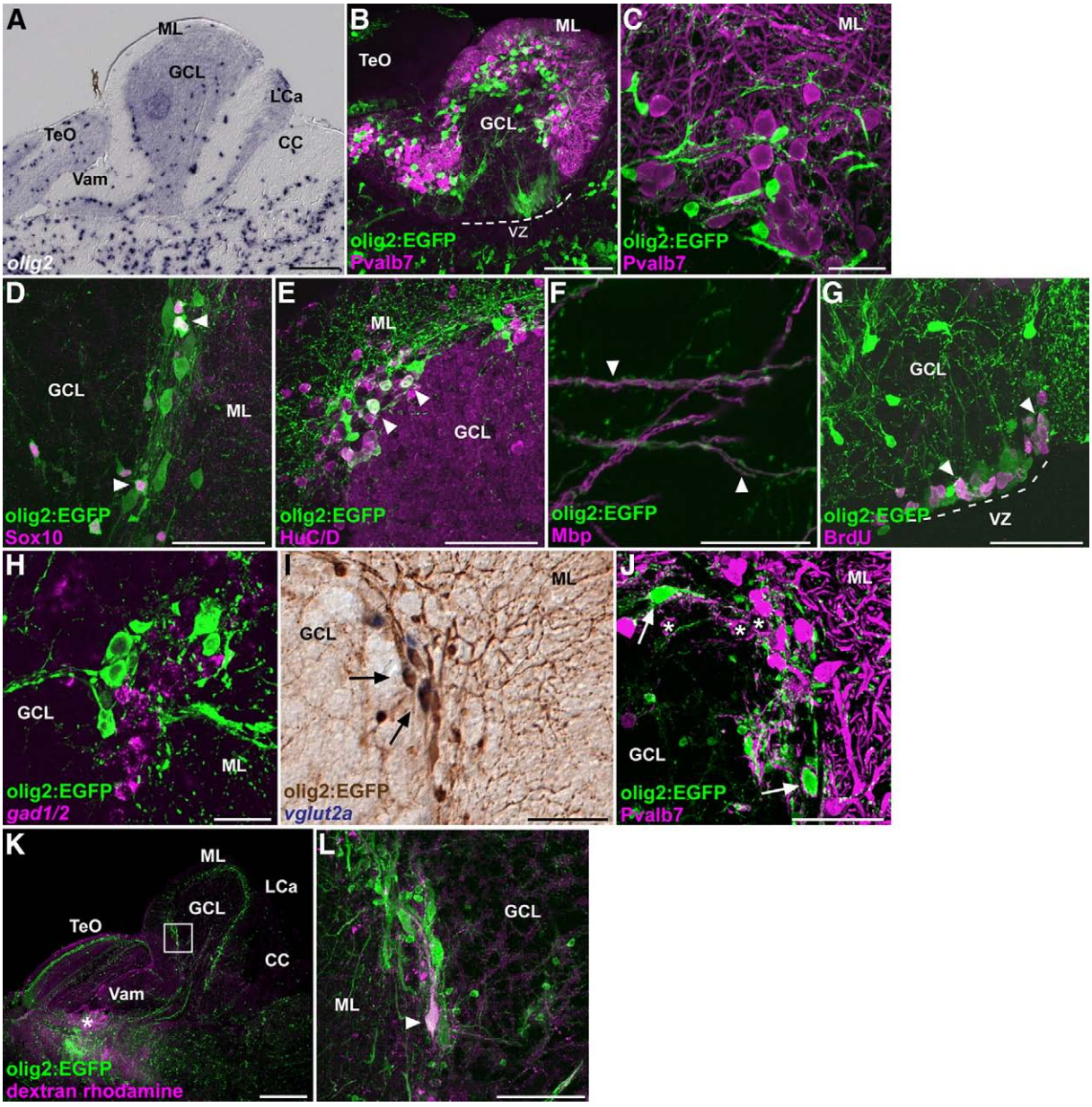

Fig. 5. *olig2*$^+$ cells. (A) Expression of *olig2* in the adult cerebellum. A sagittal section. (B, C) Co-staining of a *Tg(olig2:EGFP)* brain with anti-Pvalb7 (magenta) and anti-EGFP (green) antibodies. Low (B) and high (C) magnification views. Note that the EGFP signals never overlap with Pvalb7. The ventricular zone (VZ) is indicated by a dotted line (B). (D–F) Co-staining of the *Tg(olig2:EGFP)* brain with anti-EGFP antibodies (green), and anti-Sox10 (D), anti-HuC/D (E), or anti-Mbp (F, magenta). Sagittal sections and in the posterior CCe (D), and anterior CCe (E) and GCL (F). Note that olig2:EGFP$^+$ cells that have a small size were stained with anti-Sox10 antibody (arrowheads in D); those having a large cell size were stained with anti-HuC/D antibody (arrowheads in E). olig2:EGFP$^+$ cellular processes do not overlap with Mbp$^+$ oligodendrocytic processes, but rather are adjacent to them (arrowheads in F). (G) BrdU incorporation. Adult *Tg(olig2:EGFP)* fish were labeled with bromodeoxyuridine (BrdU) for 1 h, and the proliferating cells were analyzed by immunostaining with anti-BrdU (magenta) and anti-EGFP antibodies (green). A sagittal section. The VZ is indicated a dotted line. Note that some of olig2:EGFP$^+$ cells incorporated BrdU (arrowheads). (H) Co-staining of the *Tg(olig2:EGFP)* brain with a *gad1/gad2* riboprobe (magenta) and anti-EGFP antibody (green). olig2:EGFP signals do not overlap with *gad1/2* expression. (I) Co-staining of the *Tg(olig2:EGFP)* cerebellum with a *vglut2a* riboprobe (purple, NBT/BCIP staining) and anti-EGFP antibodies (brown, DAB staining). Note that some of the olig2:EGFP$^+$ cells express *vglut2a*. (J) Co-staining of the *Tg(olig2:EGFP)* cerebellum with anti-Pvalb7 (magenta) and anti-EGFP (green) antibodies. Note that some of olig2:EGFP$^+$ somata (arrows) receive synaptic inputs from Pvalb7$^+$ axons of Purkinje cells. The olig2:EGFP$^-$ eurydendroid cells are marked by asterisks. (K, L) Retrograde labeling of eurydendroid cells. The neural tracer was injected into the pretectal region (asterisk, K) of the *Tg(olig2:EGFP)* adult fish and the brain was stained with the fluorescent avidin (magenta) and anti-EGFP antibodies. (L) High-magnification view of the box in K. Note that an olig2:EGFP$^+$ cell (arrowhead) incorporated the neural tracer. The abbreviations are described in Fig. 1. Scale bars: 200 μm (A, B, K), 50 μm (D, E, G, I), and 20 μm (C, F, H, J, L).

We further examined the expression of *myelin basic protein* (*mbp*), a marker for oligodendrocytes (Brosamle and Halpern, 2002). The *mbp* transcripts are localized to the GCL and followed the shape of afferent or efferent tracts (Figs. 4H and I).

Characterization of olig2$^+$ neurons

olig2$^+$ neurons were recently reported to be localized to the vicinity of the PCL and to have long axons similar to those of eurydendroid cells in zebrafish (McFarland et al., 2008). We detected *olig2* transcripts in the GCL and marginally in the ML of the adult cerebellum (Fig. 5A). Using the *Tg(olig2:EGFP)* line (McFarland et al., 2008; Shin et al., 2003), we further examined the origin and characteristics of the *olig2$^+$* neurons in the adult cerebellum. The EGFP$^+$ cells in the *Tg(olig2:EGFP)* fish did not react with an anti-Pvalb7 antibody, but are located near the PCL (Figs. 5B and C). As reported for larval stages (McFarland et al., 2008), the olig2:EGFP$^+$ cells were not stained with the anti-calretinin antibody in the adult

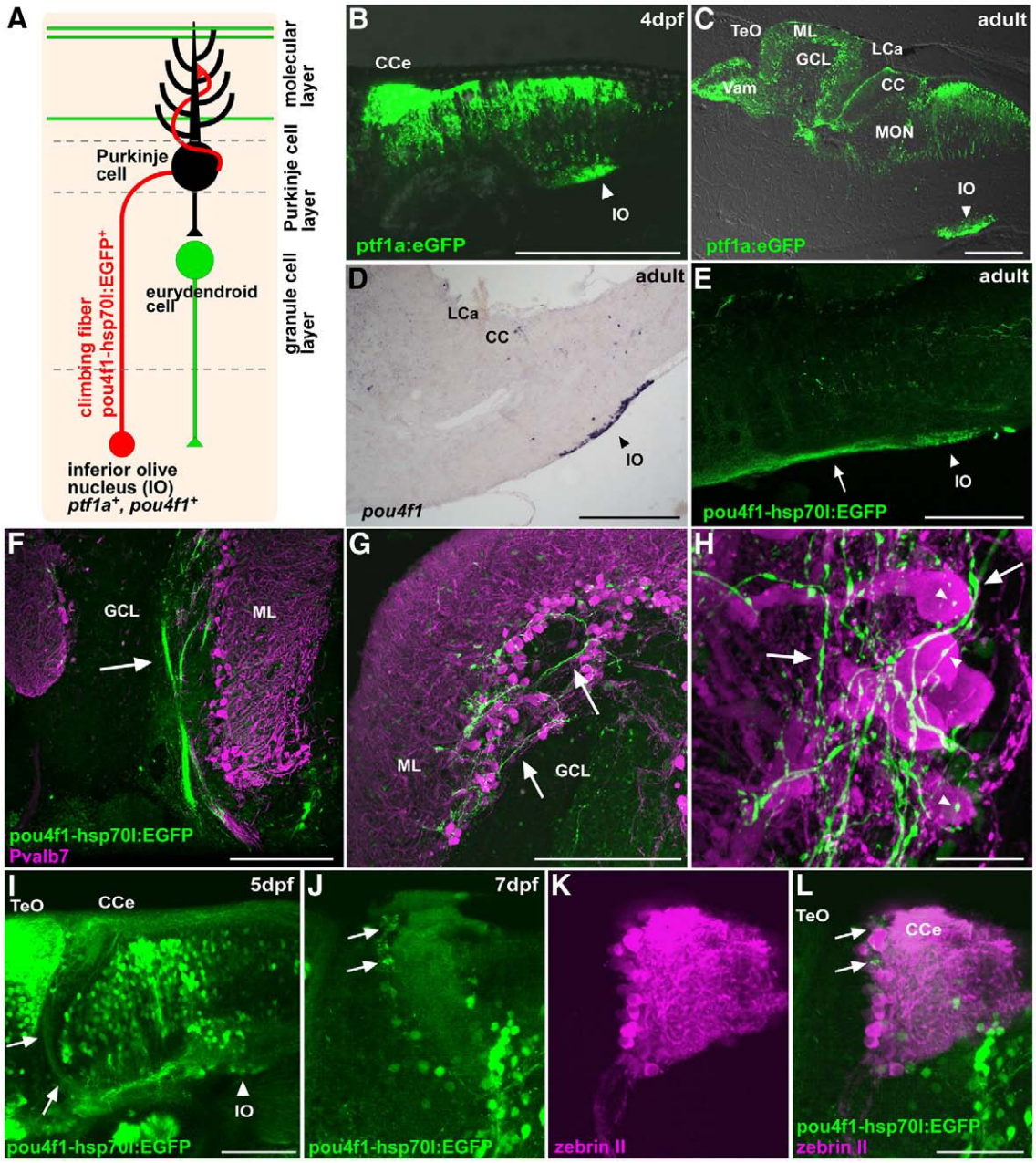

Fig. 6. Climbing fibers. (A) Schematic presentation of climbing fibers. (B, C) Detection of EGFP in the inferior olive nucleus in the *Tg(ptf1a:eGFP)* line at 4 dpf (B) and in the adult (C). Lateral view (B) and sagittal section (C), with anterior to the left. EGFP signals were detected directly with laser scanning microscopy or (B) by immunostaining with an anti-EGFP antibody (C). (D) Expression of *pou4f1 (brn3a)* in the inferior olive nucleus of the adult hindbrain. In situ hybridization of a sagittal section. (E) Staining of a *Tg(pou4f1-hsp70l:EGFP)* adult brain with the anti-EGFP antibody. EGFP signals were detected in neurons of the inferior olive nucleus (IO, arrowhead) and in their axons (indicated by an arrow). (F–H) Co-staining of the *Tg(pou4f1-hsp70l:EGFP)* brain with anti-Pvalb7 (magenta) and anti-EGFP (green) antibodies. Sagittal sections at the lateral (F) and mediolateral levels (G, H). Low (F), middle (G), and high (H) magnification views. The pou4f1-hsp70l:EGFP$^+$ climbing fibers were detected as bundles in the GCL (arrow, F), reached the PCL and ML (arrows, G, H), and synapsed on the soma (marked by arrowhead) and proximal dendrites of Purkinje cells. (I–L) Detection of pou4f1:EGFP$^+$ climbing fibers at larval stages 5 dpf (I) and 7 dpf (J–L). Immunostaining with anti-EGFP antibody (green, I); co-staining with anti-EGFP (green J, L) and zebrin II antibodies (magenta, K, L). Note that pou4f1:EGFP$^+$ climbing fibers from the inferior olive nucleus (IO, arrowhead) were detected at 5 dpf (arrows, I); they innervated to the region containing zebrin II$^+$ Purkinje cell (arrows) at 7 dpf. Lateral views with anterior to the left. Low (I) and high-magnification views (J–L). The abbreviations are described in Fig. 1. Scale bars: 200 μm (B–E), 100 μm (I), 50 μm (L, F, G), and 20 μm (H).

cerebellum (Suppl. Fig. 3), which recognizes some eurydendroid cells (Castro et al., 2006; Diaz-Regueira and Anadon, 2000; Meek et al., 2008). These olig2:EGFP$^+$ cells extend long neurites to the ML and GCL (Figs. 5B and C), as described for larval stages (McFarland et al., 2008).

olig2 is known to be expressed in oligodendrocytes and their progenitors in the spinal cord (Park et al., 2007; Zhou et al., 2000). We further examined the olig2:EGFP$^+$ cells using oligodendrocyte and neuronal markers. A small number of olig2:EGFP$^+$ cells in the GCL and near Purkinje cells have a small cell size and are positive for the oligodendrocyte marker Sox10 (Fig. 5D). However, the majority of olig2:EGFP$^+$ cells have a large cell size, and stain with the anti-HuC/D antibody (a marker for postmitotic neurons) but not with the anti-Sox10 antibody (Figs. 5D and E). The data suggest that, although olig2:EGFP$^+$ cells include oligodendrocytes, the majority of them are eurydendroid cells. Consistent with this, most of the olig2:EGFP$^+$ cellular processes do not overlap with the Mbp$^+$ oligodendrocytic processes, rather they are adjacent to them (Fig. 5F), suggesting that the olig2:EGFP$^+$ eurydendriod cell axons are surrounded by oligodendrocytic processes.

In addition, we detected EGFP$^+$ cells with protrusions that extend dorsally into the VZ (Fig. 5B), suggesting that the *olig2*$^+$ neurons originated in the VZ. Some of olig2:EGFP$^+$ cells in the VZ could incorporate BrdU (Fig. 5G), indicating that they are proliferating cells. Although inhibitory neurons (GABAergic and glycinergic) are generated from *ptf1a*$^+$ neuronal progenitors in the VZ (Hoshino, 2006; Hoshino et al., 2005), the *olig2*$^+$ (EGFP$^+$) neurons do not express *gad1*, *gad2*, *glyt1*, or *glyt2* (Fig. 5H, data not shown for *glyt1/2*). Moreover, we found that at least some of the *olig2*$^+$ (EGFP$^+$) neurons express *vglut2a* (Fig. 5I) and receive inputs from Purkinje cell axons (Fig. 5J), suggesting that at least a portion of the *olig2*$^+$ neurons function as eurydendroid cells. To address this issue, we carried out retrograde labeling of the eurydendroid cells by injecting a neural tracer (dextran, teteramethylrhodamine and biotin) into the pretectal region (Fig. 5K), where many eurydendroid cells send their axons (Ikenaga et al., 2005). We found that some of the retrogradely labeled cells were olig2:EGFP$^+$ (Fig. 5L), confirming that at least a number of *olig2*$^+$ neurons are eurydendroid cells. The cell-specific markers for zebrafish cerebellum are summarized in Table 1.

Characterization of afferent and efferent tracts

The cerebellum receives inputs from two different types of afferent fibers (Figs. 6A and 7A). The climbing fibers are axons from the IO (Fig.

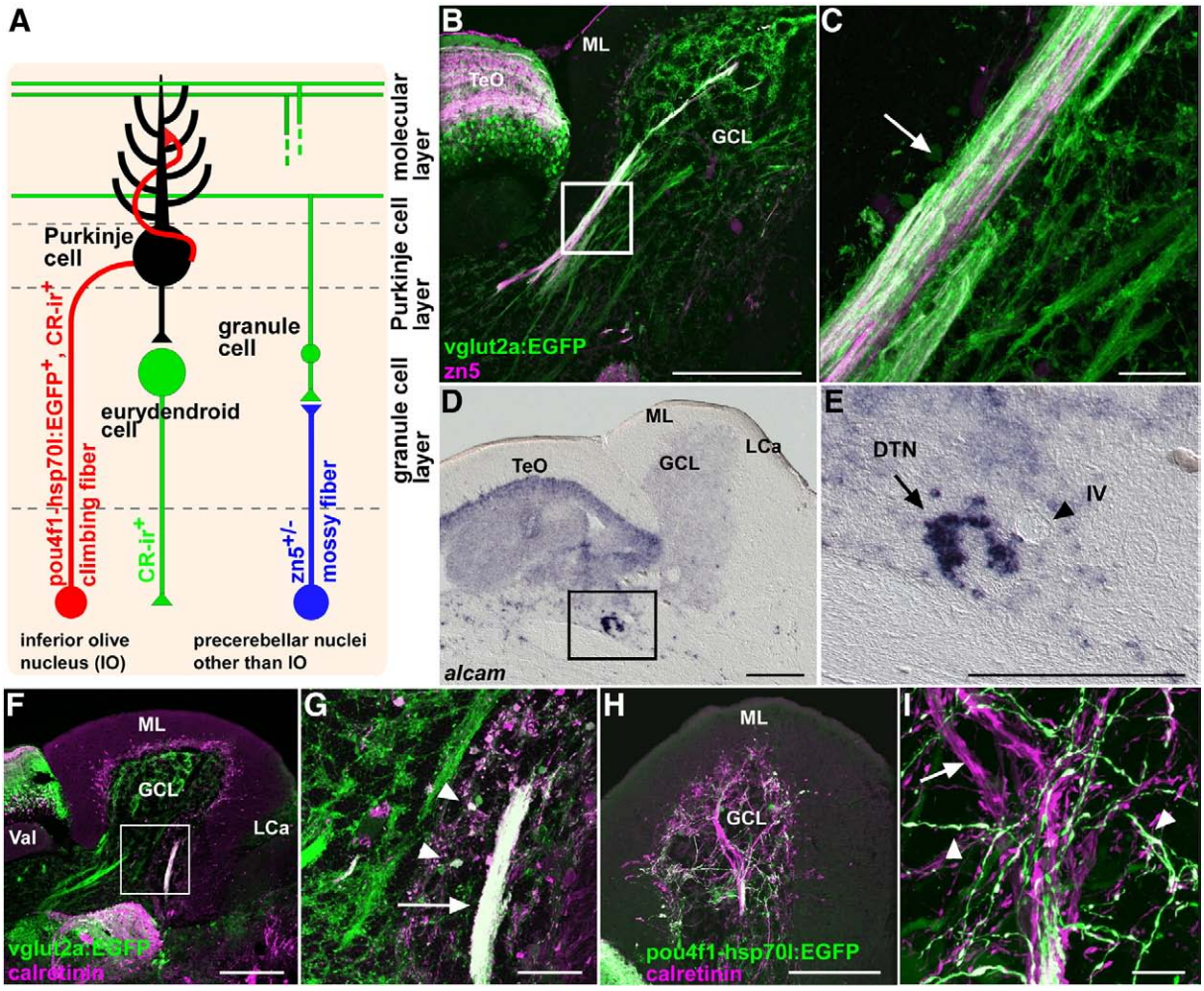

Fig. 7. Mossy fibers and efferent fibers from eurydendroid cells. (A) Schematic presentation of mossy fibers and efferent fibers. (B, C) Co-staining of a *Tg(vglut2a:EGFP)* brain with zn5 (magenta) and anti-EGFP (green) antibodies. (C) High-magnification view of the box in B. The zn5$^+$ vglut2a:EGFP$^+$ mossy fibers are indicated by an arrow. (D, E) Expression of *alcam (zn5)*. (E) High-magnification view of the box in D. The *alcam*-expressing cells (marked by an arrow) are located in the vicinity of the trochlear nerve (IV, marked by an arrowhead). (F, G) Co-staining of the *Tg(vglut2a:EGFP)* brain with anti-calretinin (magenta) and anti-EGFP (green) antibodies. (G) High-magnification view of the box in F. The anti-calretinin antibody stained the soma (arrowheads) and efferent axons (arrow) of eurydendroid cells (vglut2a:EGFP$^+$). (H, I) Co-staining of a *Tg(pou4f1-hsp70l:EGFP)* brain with anti-calretinin (magenta) and anti-EGFP (green) antibodies. All of the pou4f1-hsp70l:EGFP$^+$ axons were stained with the anti-calretinin antibody (arrowheads, climbing fibers). Calretinin-immunoreactive pou4f1-hsp70l:EGFP$^-$ tracts (arrows) are the axons of eurydendroid cells. F/G and H/I show mediolateral and lateral sections, respectively. The abbreviations are described in Fig. 1. Scale bars: 200 μm (B, D, E, F, H, J), 50 μm (G), and 20 μm (C, I).

Table 2
Neural tracts.

Tract	Origin	Synaptic terminal	Markers
Afferent fibers			
Climbing fibers	Inferior olive nucleus	Soma and proximal dendrites of PC	pou4f1-hsp70l:EGFP$^+$, CR-ir$^+$, vglut2a:EGFP$^+$
Mossy fibers*[1]	Dorsal tegmental nuclei	Cerebellar glomeruli	zn5$^+$, vglut2a:EGFP$^+$
Mossy fibers*[2]	Pre-cerebellar nuclei	Cerebellar glomeruli	zn5$^-$, CR-ir$^-$, olig2:EGFP$^-$, vglut2a:EGFP$^+$
Efferent fibers			
Axons of eurydendroid cells	Eurydendroid cells	?	pou4f1-hsp70l:EGFP$^-$, CR-ir$^+$, vglut2a:EGFP$^+$
Axons of unconventional eurydendroid cells	*olig2*$^+$ eurydendroid cells	?	olig2:EGFP$^+$, CR-ir$^-$, vglut2a:EGFP$^+$*[3]
Cerebellovestibular tracts	PC	Vestibular nuclei	Pvalb7$^+$, zebrin II$^+$
Inner circuits			
Granule cells' axons (parallel fibers)	Granule cells	Dendrites of PC and GI	Vglut1$^+$
Interneurons' axons	GI	Dendrites of PC	Gad1$^+$ in ML
Golgi axons	Golgi cells	Cerebellar glomeruli	Gad1$^+$ in GCL

CR-ir, anti-calretinin antibody-immunoreactive; GCL, granule cell layer; GI, GABAergic interneurons (stellate cells); ML, molecular layer; PC, Purkinje cells. *[1,2]Mossy fibers from the dorsal tegmental nuclei were identified by zn5 staining*[1], but there was no specific marker found for the pre-cerebellar neurons of other mossy fibers*[2]. *[3]Some of the *olig2*$^+$ neurons were *vglut2a*^{high} glutamatergic neurons, and the localization of their axonal terminal was not identified.

6A). Tracing experiments in other teleost species have demonstrated a connection between the CCe and the IO that corresponds to the climbing fibers (Folgueira et al., 2006; Wullimann and Northcutt, 1988, 1989). In mammals, the IO neurons are reported to be derived from *Ptf1a*-expressing neuronal progenitors in the hindbrain (Yamada et al., 2007) and to express the homeobox gene *Pou4f1 (Brn3a)* (Fedtsova and Turner, 1995). Using *Tg(ptf1a:eGFP)* (Godinho et al., 2007; Pisharath et al., 2007) and *Tg(pou4f1-hsp70l:EGFP)* fish (Aizawa et al., 2005), we examined the localization and morphology of the IO neurons in zebrafish larvae and adult fish (Fig. 6). EGFP$^+$ cells in the *Tg(ptf1a:eGFP)* line were detected in the IO, which is located in the ventro-medial region of the posterior hindbrain, at 4 dpf (Fig. 6B), and the EGFP expression continued into adulthood (Fig. 6C), suggesting a conserved role for Ptf1a in the development of the IO. Just as *pou4f1 (brn3a)* is expressed in the IO of adult fish (Fig. 6D), EGFP$^+$ (pou4f1-hsp70l:EGFP$^+$) cells in the *Tg(pou4f1-hsp70l:EGFP)* adult fish were also detected in the IO, and they extended their axons anteriorly (Fig. 6E). The co-staining of serial sections with the anti-Pvalb7 antibody revealed that the pou4f1-hsp70l:EGFP$^+$ fibers form thick bundles in the GCL (Fig. 6F), and innervate the soma and proximal dendrites of Purkinje cells (Figs. 6G, H), which are characteristic features of climbing fibers. We detected pouf41-hsp70l:EGFP$^+$ climbing fibers that innervate the cerebellum from 5 dpf (Figs. 6I, J, K, L). This is consistent with the recent report that shows detection of the climbing fibers 5 dpf with the *hoxb4a-YFP* enhancer trap line (Punnamoottil et al., 2008).

vglut2a/b are expressed in both climbing and mossy fiber neurons outside the cerebellum, and in eurydendroid cells within it (Figs. 3D

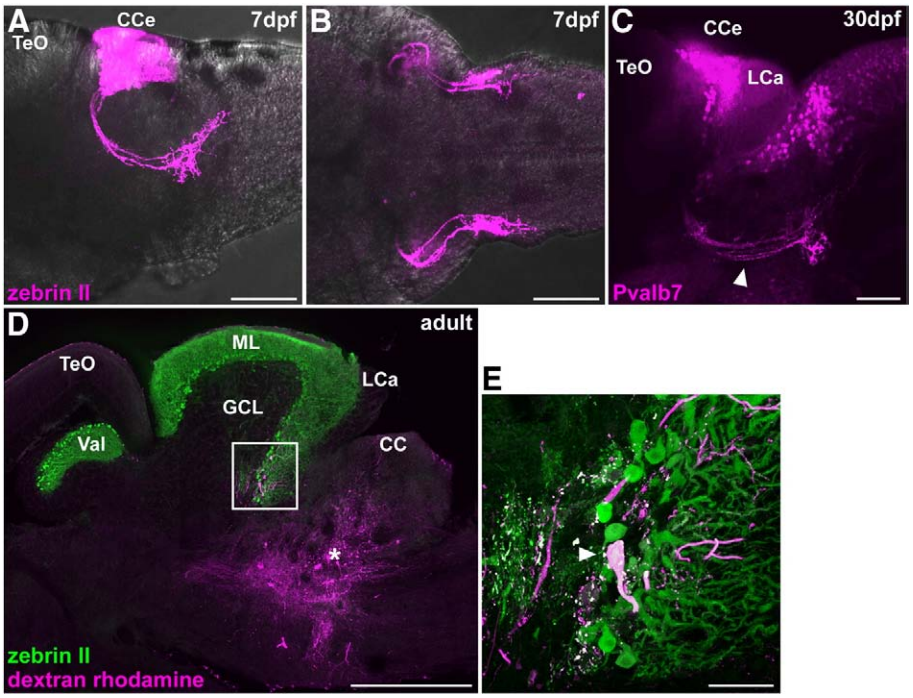

Fig. 8. Cerebellovestibular tracts. (A, B) Immunostaining of 7 dpf larval brains with zebrin II. Lateral (A) and ventral (B) views with anterior to the left. (C) Immunostaining of a 30 dpf juvenile fish brain with anti-Pvalb7 antibody. Lateral view with anterior to the left. Cerebellovestibular tracts are indicated by arrowhead. (D, E) Retrograde labeling of cerebellovestibular tracts. A biotin-conjugated neural tracer was injected to the vestibular region (asterisk, D), which includes the descending octaval nucleus, of adult fish. A sagittal section was stained with zebrin II (green) and fluorescently labeled avidin (magenta). (E) High-magnification view of the box in (D). Note that a retrogradely labeled cell is a zebrin II$^+$ Purkinje cell. The abbreviations are described in Fig. 1. Scale bars: 500 μm (D), 100 μm (A–C) and 50 μm (E).

and E). We raised *Tg(vglut2a:EGFP)* transgenic fish and examined them with an anti-Vglut2a antibody, to detect the axons and axonal terminals of *vglut2*$^+$ glutamatergic neurons. The EGFP$^+$ (vglut2a:EGFP$^+$) axons were detected as bundles in the GCL of the *Tg(vglut2a:EGFP)* adult cerebellum. We found that some of the vglut2a:EGFP$^+$ axons are co-stained with zn5 (Figs. 7B and C) or anti-calretinin (Figs. 7F and G) antibodies. The zn5 antibody recognizes Alcam (activated leukocyte cell adhesion molecule, also known as DM-GRASP) (Kanki et al., 1994). The *alcam*-expressing cells are located in the dorsal tegmental nucleus (Figs. 7D and E), and they extend vglut2a:EGFP$^+$/zn5$^+$ axons to the GCL (Fig. 7B), indicating that these axons are mossy fibers. The anti-calretinin antibody recognizes eurydendroid cells, the IO neurons, the pretectal nuclei (mossy fiber neurons), and their neurites (Castro et al., 2006; Diaz-Regueira and Anadon, 2000; Meek et al., 2008) (Suppl. Fig. 3). It reacted with the vglut2a:EGFP$^+$ somata and axons (eurydendroid cells, Fig. 6G) and with pou4f1-hsp70l:EGFP$^+$ axons (climbing fibers, Figs. 7H and I). Thus, the vglut2a:EGFP$^+$ fibers can be classified into five different neurons and neuronal tracts: (1)

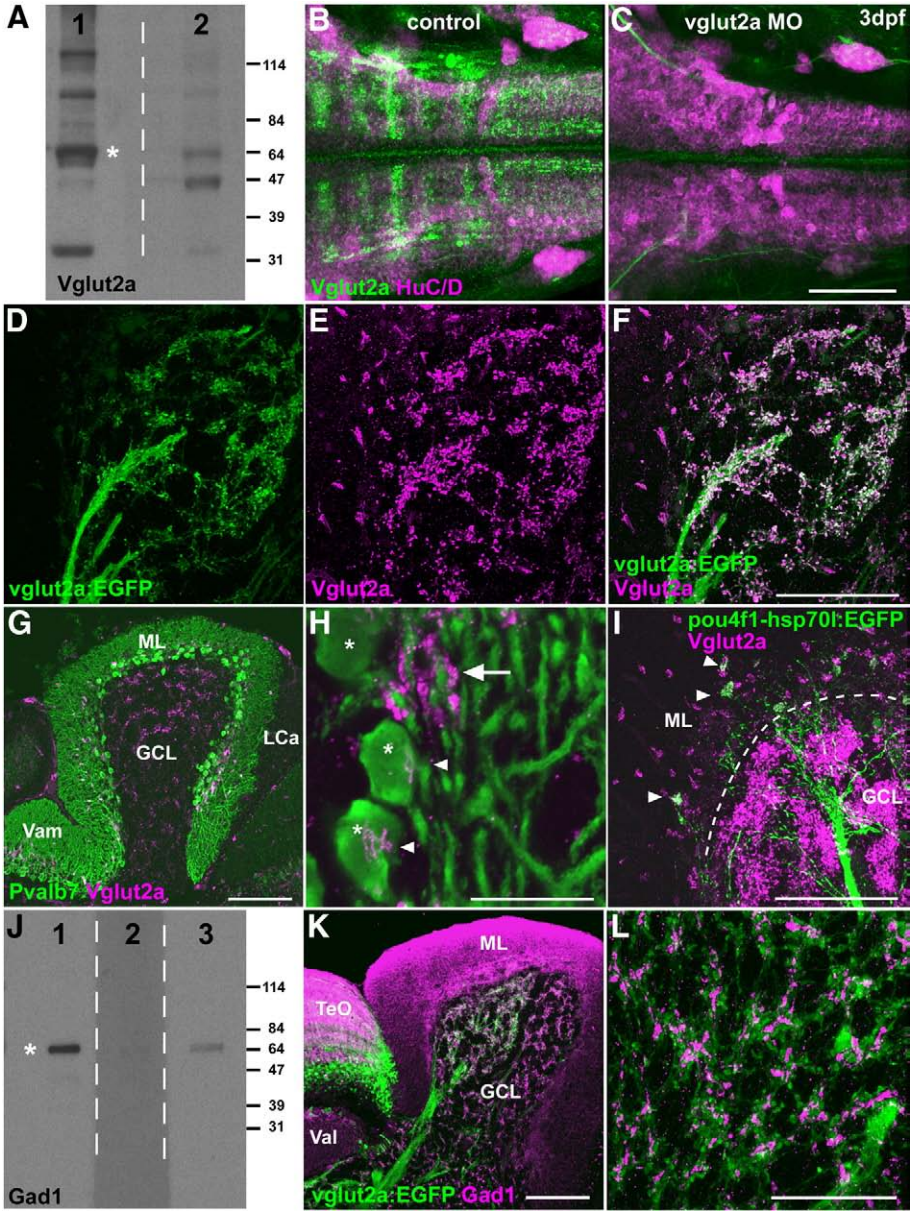

Fig. 9. Presynaptic terminals of mossy and climbing fibers. (A) Immunoblotting of brain lysates with an anti-Vglut2a antibody. Rabbit anti-Vglut2a (lane 1) and pre-immune sera (lane 2) were used to detect Vglut2a (asterisk). Several bands other than 64-kD Vglut2a were detected in lane 1, but they are likely non-specific as they were also detected in lane 2. (B, C) Immunostaining of Vglut2a. Larva at 3 dpf that received 4 pg of antisense *vglut2a* MO (C) and control larva (B) stained with anti-Vglut2a (green) and anti-HuC/D (magenta) antibodies. Dorsal views of the hindbrain regions. Anti-Vglut2a but not anti-HuC/D staining was abolished in the *vglut2a* morphant hindbrain. (D–F) Co-staining of a *Tg(vglut2a:EGFP)* brain with anti-Vglut2a and anti-EGFP antibodies. EGFP (green, D), Vglut2a (magenta, E) and merged images (F) are shown. Sagittal section. Note that Vglut2a$^+$ dots are detected in the distal tips (presynaptic terminals) of vglut2a:EGFP$^+$ axons (mossy fibers) in the GCL. (G, H) Co-staining with anti-Vglut2a (magenta) and anti-Pvalb7 (green) antibodies. Low (G) and high (H) magnification views. Vglut2a$^+$ synaptic boutons were detected on the soma (arrowheads) of Purkinje cells (asterisks) or abutting the proximal dendrites of Purkinje cells (arrow). (I) Co-staining of *a Tg(pou4f1-hsp70l:EGFP)* brain with anti-Vglut2a (magenta) and anti-EGFP (green) antibodies. Vglut2a$^+$ dots were also pou4f1:EGFP$^+$ in the ML (arrowheads), indicating they were presynaptic terminals of climbing fibers. The position of the PCL is indicated by a dotted line. (J) Immunoblotting of brain lysates with anti-Gad1 antibodies. Rabbit anti-Gad1 generated in this study (lane 1), control sera (pre-immune sera, lane 2), and commercially available anti-human GAD1/2 (lane 3) were used to detect zebrafish Gad1 (asterisk). (K, L) Co-staining of the *Tg(vglut2a:EGFP)* brain with anti-Gad1(magenta) and anti-EGFP (green) antibodies. Low (K) and high (L, in GCL) magnification views. Vglut2a$^+$ and Gad1$^+$ dots were adjacent in the GCL and indicated the cerebellar glomeruli. The abbreviations are as described in Fig. 1. Scale bars: 100 μm (C, F, G, I, K), 50 μm (L), and 20 μm (H).

zn5$^+$ mossy fibers from the dorsal tegmental nuclei; (2) calretinin-immunoreactive (CR-ir$^+$) and pou4f1-hsp70l:EGFP$^+$ climbing fibers; (3) CR-ir$^+$ and pou4f1-hsp70l:EGFP$^-$ eurydendroid cell axons; (4) olig2:EGFP$^+$ (CR-ir$^-$) eurydendroid cell axons; and (5) other marker-negative mossy fibers (Table 2).

In addition, we labeled the cerebellovestibular tracts (Fig. 8): direct efferent fibers from the Purkinje cells to the neurons of the vestribular nuclei, which are also found in mammals (Altman and Bayer, 1997). Both anti-Pvalb7 and anti-zebrin II stainings revealed extracerebellar projections from the Purkinje cells, which are located in the lateral part of the CCe, at larval and juvenile stages (Figs. 8A, B, C). Following the application of a neural tracer to the vestibular region (Fig. 8D), including the DON of the adult brain, we detected the tracer in zebrin II$^+$ Purkinje cells (Fig. 8E), confirming the presence of the cerebellovestibular tracts.

Synaptic terminals of climbing and mossy fibers

The anti-Vglut2a antibody recognized the 64-kD Vglut2a protein (Fig. 9A) and specifically stained the Vglut2a$^+$ neurons in the embryonic hindbrain (Higashijima et al., 2004a), since the injection of antisense MOs against *vglut2a* abrogated the anti-Vglut2a staining (Figs. 9B and C). Vglut2a$^+$ dots are detected in the distal tips of vglut2a:EGFP$^+$ axons in the GCL (Figs. 9D, E, and F), suggesting that they correspond to the presynaptic terminals of the *vglut2*$^+$ glutamatergic neurons. Vglut2a$^+$ dots were also detected on the soma of Purkinje neurons or abutting the proximal dendrites of Purkinje cells (Figs. 9G and H), and some of these Vglut2a$^+$ dots are also pou4f1-hsp70l:EGFP$^+$ (Fig. 9I), indicating that some of the Vglut2a$^+$ dots mark the presynaptic terminals of the climbing fibers in the ML.

The mossy fibers terminate on the dendrites of granule cells where the axons of GABAergic Golgi cells contact the dendrites of granule cells to form the cerebellar glomeruli. We raised an anti-zebrafish Gad1 antibody that recognized the 65-kD Gad1 protein in zebrafish brain lysates (Fig. 9J) and stained the presynaptic terminals of GABAergic neurons in the ML and GCL (Fig. 9K), as did an anti-human/mouse GAD1/2 antibody (data not shown). The Vglut2a$^+$ and Gad1$^+$ dots are adjacent to each other in the GCL, where they form clusters (Fig. 9L), suggesting that the clusters are cerebellar glomeruli in which the axons of the *vglut2*$^+$ mossy fibers and *gad1*$^+$ Golgi cells meet with the dendrites of granule cells (Castejon et al., 2000).

Neural connections within the cerebellum

To examine the axons (parallel fibers) of granule cells (Fig. 10A), we raised antibodies against Vglut1. Although *vglut1* is expressed specifically in the granule cells in the GCL (Fig. 3A), Vglut1 was not detected in the GCL but in the ML (Fig. 10C), confirming that Vglut1 is located in the presynaptic terminals of granule cells (Boulland et al., 2004). Vglut1$^+$ dots abut both the proximal and distal regions of the Pvalb7$^+$ dendrites of Purkinje cells (Figs. 10D and E). Similarly, we also detected Gad1$^+$ dots close to the Pvalb7$^+$ dendrites of Purkinje cells (Figs. 10F and G), indicating that they mark the presynaptic terminals of GABAergic interneurons, including stellate cells. Gad1$^+$ dots were also detected on the soma of Purkinje cells (Fig. 10G). These may be the presynaptic terminals of Purkinje cells, as Purkinje cells send their axons to other neighboring Purkinje cells (Bell et al., 2008; Butler and Hodos, 1996).

Cerebellum-like structures

We further examined the expression of Pvalb7 and Vglut1 in the cerebellum-like structures in the optic tectum and anterior hindbrain: TL-SM-Type I neuron circuitry and EG-CC-MON circuitry

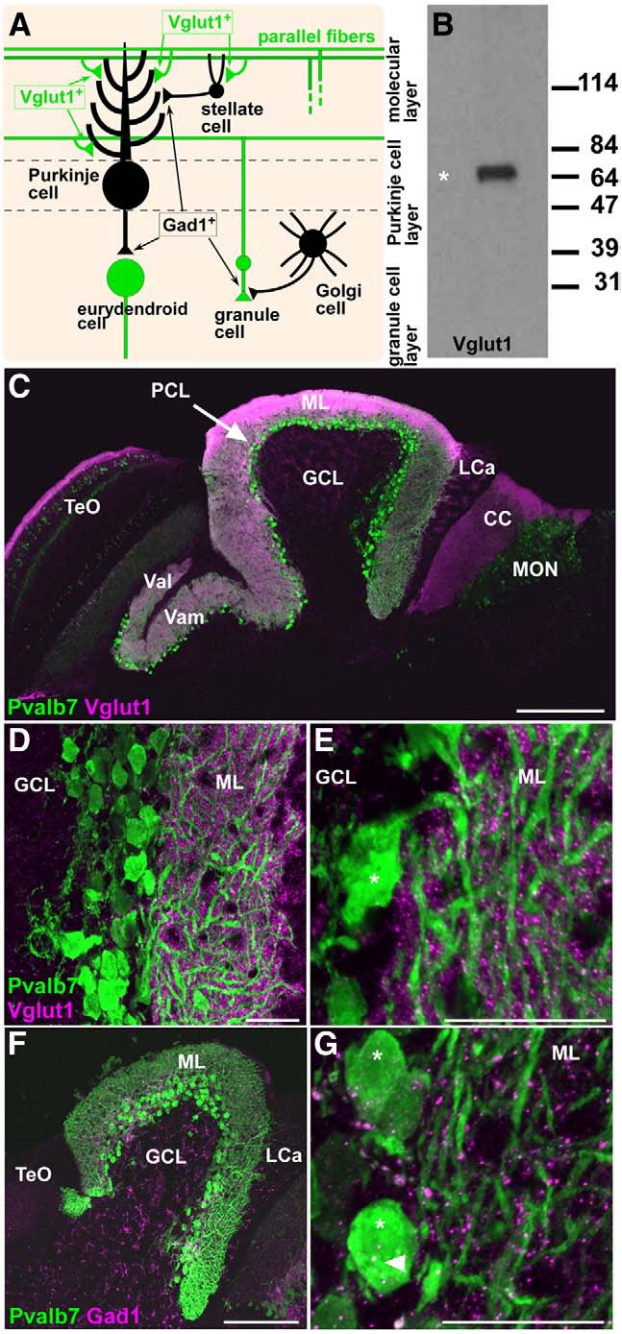

Fig. 10. Presynaptic terminals of granule neurons (parallel fibers) and GABAergic interneurons. (A) Schematic presentation. (B) Immunoblotting of brain lysates with the anti-Vglut1 antibody. (C–E) Co-staining with anti-Pvalb7 (green) and anti-Vglut1 (magenta) antibodies. (C–E) Sagittal sections with anterior to the left; low (C), medium (D), and high (E) magnification views. (D, E) Corpus cerebelli (CCe). Vglut1$^+$ dots (presynaptic boutons of parallel fibers) abutted the dendrites but not the soma (asterisk) of Purkinje cells in the ML. (F, G) Co-staining with anti-Pvalb7 (green) and anti-Gad1 (magenta) antibodies. Gad1$^+$ dots (presynaptic boutons of GABAergic interneurons) abut the dendrites and somata (asterisks) of Purkinje cells. The abbreviations are as described in Fig. 1. Scale bars: 200 μm (C), 100 μm (F) and 20 μm (D, E, G).

(Fig. 11). Pvalb7 was detected in the soma, dendrites, and axon of the Purkinje-like cells of these structures: type I neurons in the TeO (Fig. 11A) and crest cells in the MON (Fig. 11D). These Pvalb7$^+$ dendrites co-localize with the Vglut1$^+$ presynaptic terminals in the stratum marginale (SM, Figs. 11B and C) of the TeO and CC (Figs. 11E and F), indicating that Pvalb7 and Vglut1 are also utilized in these

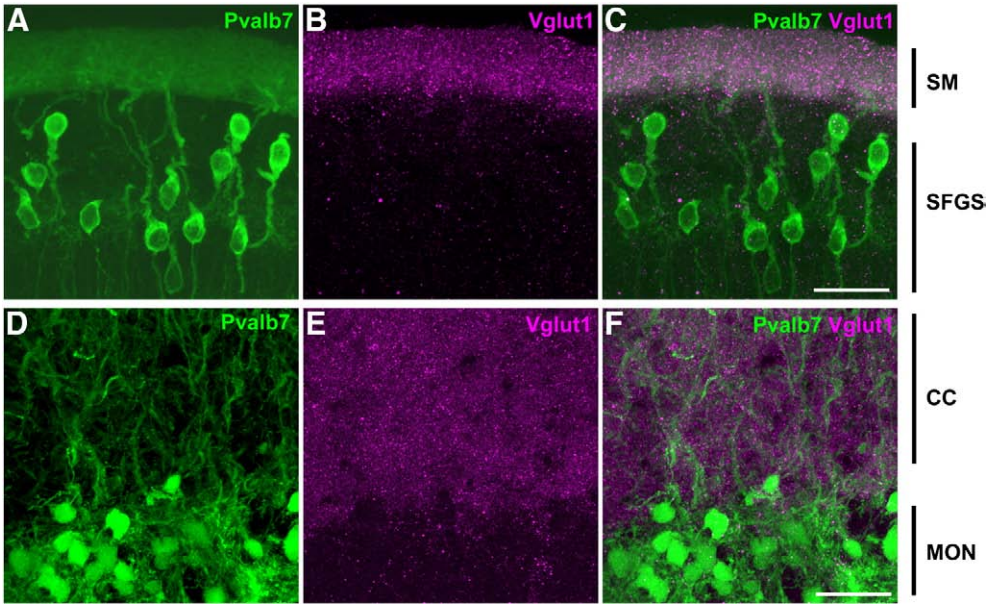

Fig. 11. Cerebellum-like structures. Co-staining of anti-Pvalb7 (green) and anti-Vglut1 (magenta) antibodies in the cerebellum-like structures in the optic tectum and antero-dorsal hindbrain: the TL-SM-type I neuron (A–C) and EG-CC-MON circuitries (D–F). Sagittal sections with dorsal to the top. Pvalb7 (A, D) and Vglut1 (B, E) signals and merged images (C, F) are shown. In the TL-SM-type I neuron circuitry, Pvalb7 is expressed in type I neurons in the stratum fibrosum et griseum superficiale (SFGS) of the torus longitudinalis (TL) and their dendrites in the stratum marginale (SM, J), and Vglut1 was detected in the SM. Note that morphology of type I neurons is different from Purkinje cells in the cerebellum: type I neurons have one long primary dendrite that branches far from the soma. A primary dendrite of some type I neurons is not observed because of the plane and width of the section (A). In the EG-CC-MON circuitry, Pvalb7 was detected in the crest cells in the MON and their dendrites in the CC, and Vglut1 was detected in the CC. Other abbreviations are described in Fig. 1. Scale bars: 20 μm.

cerebellum-like structures. The neural tracts are summarized in Table 2.

Development of the cerebellum in zebrafish larvae

Using molecular markers characterized in this study, we examined the development of Purkinje and granule cells, and their neurites, at larval stages of the zebrafish (Fig. 12). The expression of *pvalb7* and *aldocl* was first detected in the medial region of the cerebellum in 3-dpf larvae (Fig. 12A, data not shown for *aldocl*), indicating that the differentiation of Purkinje cells is initiated at this stage. The expression of *gad1* and *gad*2 was also detected in the cerebellum from 3 dpf (data not shown). The expression of *vglut1* was initially detected at 3 dpf in the lateral regions of the cerebellum (Fig. 12E′), which correspond to the prospective EG (Figs. 12F and G). *vglut1* was also detected in the antero-medial regions (Fig. 9E) at 3.5 dpf, which give rise to the CCe (and possibly Va) (Fig. 12G). *vglut1* expression was then observed in the granule cells at the posterior edge, at 5 dpf, which correspond to the prospective LCa (Fig. 12F), revealing that the differentiation of granule cells in the LCa begins later than that of granule cells in the EG and CCe. The number of *pvalb7*$^+$ Purkinje cells and *vglut1*$^+$ granule cells increases continuously (Figs. 12B and F), and, at 5 dpf, *vglut1*$^+$ granule cells were detected beneath the PCL in the CCe, but were located superficially in the lateral regions (Fig. 12L), indicating the formation of the GCL in the EG and CCe.

Immunostaining of the larval cerebellum (Figs. 12I, J, and K) revealed that the Purkinje cells extend Pvalb7$^+$ dendrites dorsally in the anterior CCe (Figs. 12Ia and Ka) and posteriorly in the posterior CCe (Figs. 12Ib and Kb), and these dendrites co-localize with the Vglut1$^+$ presynaptic terminals of the parallel fibers (Figs. 12Ja, Ka, Jb, and Kb) at 5 dpf. These findings indicate that the ML forms by 5 dpf. The Vglut1$^+$ parallel fibers also show extensions posterior to the CCe at 5 dpf (Figs. 12J and K). The lobular structure, consisting of the Va, CCe, EG, and LCa, is evident from 10 dpf (Figs. 12C, D, G, and H). Thus, cerebellar neurons begin to differentiate at around 3 dpf, and the layered structure starts to form at around 5 dpf.

Mutations affecting the development of the cerebellum

To reveal genetic cascades that control cerebellar development, we screened zebrafish mutants for defects in the development of Purkinje and granule cells and in the formation of their neurites. We generated F2 families from ENU-treated male fish, crossed the F2 animals to obtain F3 embryos, and reared them until 5 dpf. These larvae were stained with anti-Pvalb7 and anti-Vglut1 antibodies, which respectively recognize the Purkinje cell structure and granule cell axons (Figs. 13C, D, E). Mutations affecting the number and/or morphology of Pvalb7$^+$ Purkinje cells and/or Vglut1$^+$ granule cells' axons were selected and subjected to further analyses. We screened 826 mutated genomes, and isolated nine mutants, which were categorized into five groups (Table 3).

Group A mutants showed defects in the formation of the mid-hindbrain boundary at 3 dpf. One mutation in group A (*rk9*) was found to be allelic to *pax2a (no isthmus)* by complementation analysis, validating our screening strategy. Group B and C mutants displayed a reduced or no expression of Pvalb7 and Vglut1; group C mutants showed severe abnormalities in the development of other tissues, whereas group B mutants showed minimal or no discernible phenotypes in other tissues. *evanescence* (*eva*) mutants in group B had no apparent phenotypes before 4 dpf, but showed nearly complete loss of Purkinje cells and granule cell axons at 5 dpf (Figs. 13H, I, and J); they also had small eyes (Fig. 13G). *asynergy* (*asy*) and *drunken sailor* (*drs*) mutants in group B showed a strong reduction or loss of granule cell axons but a mild reduction of Purkinje cells at 5 dpf (Figs. 13M, N, and O). In these mutant larvae, the Purkinje cells were organized into a thin line (there are no Purkinje cells in the prospective Va), and the formation of the Purkinje cell dendrites was strongly perturbed (Fig. 13M). In addition, the *asy* and *drs* mutants had a slightly small head and a dorsally curved tail (Figs. 13K and L). Group D mutants showed a specific loss in the granule cell axons (*gazami (gaz)*, Figs. 13P–T). Group E mutants showed defects in neurite formation but not in the specification of Purkinje and granule cells. In the *shiomaneki (sio)*

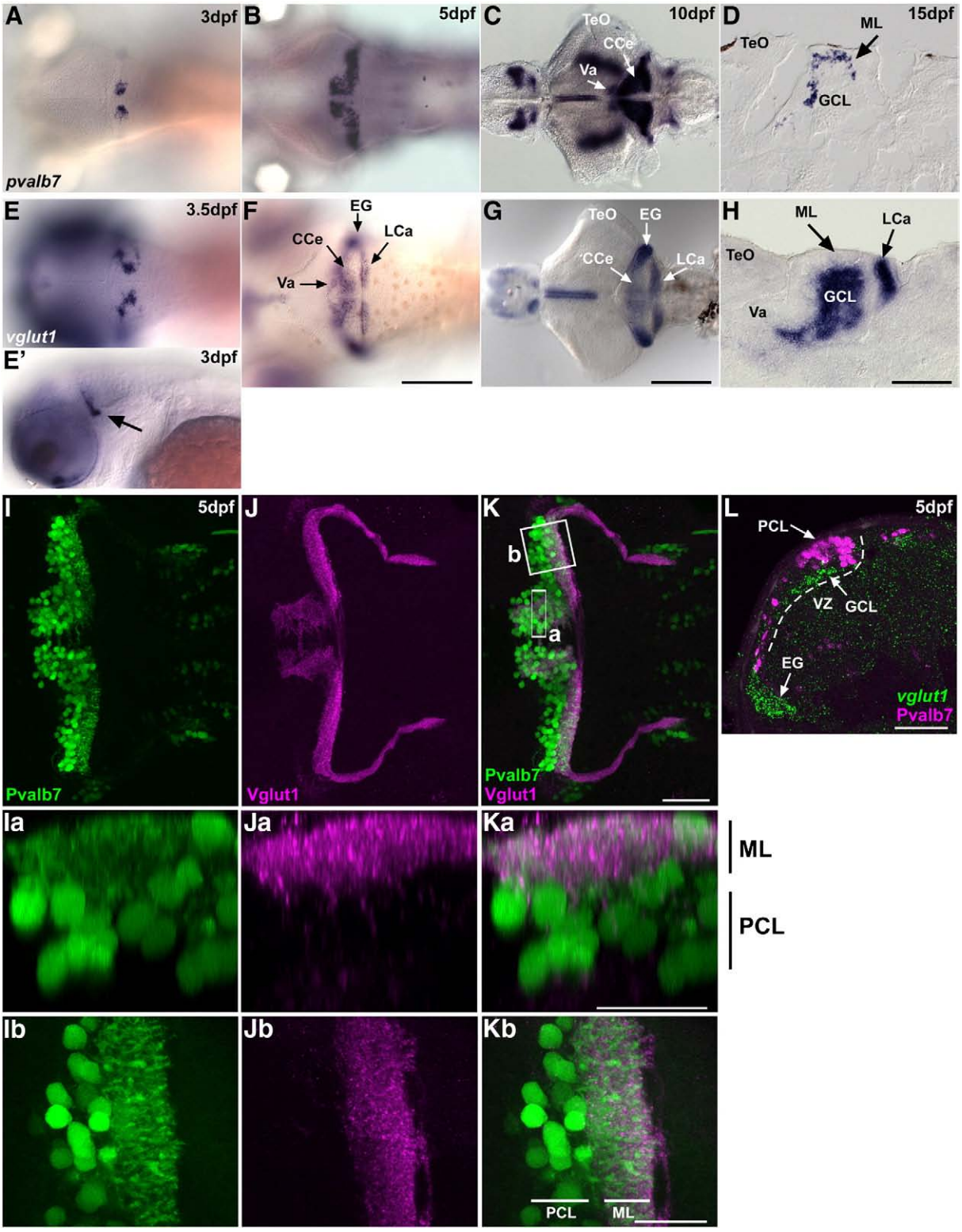

Fig. 12. Development of the cerebellum at larval stages. (A–D) Expression of *parvalbumin7* (*pvalb7*) at 3 dpf (A), 5 dpf (B), 10 dpf (C), and 15 dpf (D). (E–H) Expression of *vglut1 (slc17a7)* at 3.5 dpf (E), 5 dpf (F), 10 dpf (G), and 15 dpf (H). Dorsal views (A–C, E–G), lateral view at 3 dpf (E′), and sagittal sections (D, H). (I–K) Co-staining of 5-dpf larvae with anti-Pvalb7 (green) and anti-Vglut1 (magenta) antibodies. Pvalb7 (I, Ia, Ib) and Vglut1 (J, Ja, Jb) signals and merged images (K, Ka, Kb) are shown. (I–K) Dorsal views with anterior to the left. (Ia–Ka) Transverse-section images of box a in K generated by *Z*-stack data, with dorsal to the top. (Ib–Kb) High-magnification view of box b in K, with anterior to the left. Pvalb7$^+$ dendrites extended to the ML dorsally (Ka) and posteriorly (Kb), and interacted with Vglut1$^+$ presynaptic terminals of the parallel fibers at 5 dpf. (L) Co-staining 5-dpf cerebellum with a vglut1 riboprobe (green) and anti-Pvalb7 antibody (magenta). Transverse section with dorsal to the top. The ventricular zone (VZ) is indicated by a dotted line. The *vglut1*$^+$ granule cell layer (GCL) formed beneath the Purkinje cell layer (PCL) by 5 dpf. EG, eminentia granularis; other abbreviation are described in Fig. 1. Scale bars: 500 μm (G), 200 μm (F), 100 μm (H), and 50 μm (K, Ka, Kb, L).

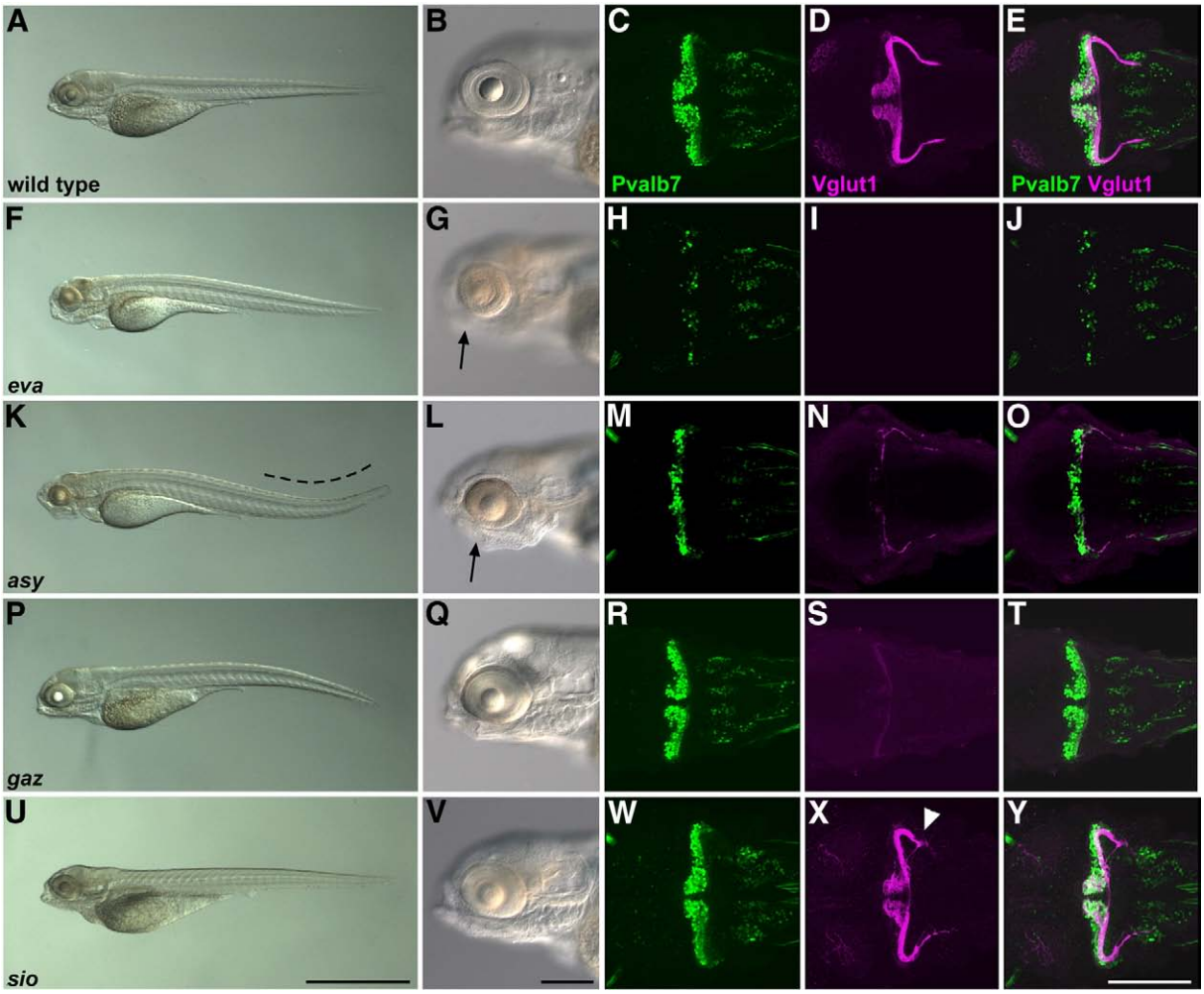

Fig. 13. Cerebellar mutants. (A–E) Wild-type, (F–J) *evanescence* (*eva*), (K–O) *asynergy* (*asy*), (P–T) *gazami* (*gaz*), and (U–Y) *shiomaneki* (*sio*) mutant larvae at 5 dpf. The embryos and larvae were treated with phenylthiourea to prevent pigmentation. The fixed 5-dpf larvae were stained with anti-Pvalb7 and Vglut1 antibodies. Bright-field images of the entire body (A, F, K, P, U) and the head region (B, G, L, Q, V). Lateral views with anterior to the left. Pvalb7 immunostaining (green; C, H, M, R, W), Vglut1 immunostaining (magenta; D, I, N, S, X), and merged images (E, J, O, T, Y). Dorsal views with anterior to the left. The *eva* and *asy* mutants had small eyes (indicated by arrows). Scale bars: 1 mm (U) and 200 μm (V, Y).

mutants in Group E, the granule cell Vglut1$^+$ axons that extended to the CC were shortened (Figs. 13X and Y). Mutants in Group D/E did not show any apparent abnormalities in the development of other tissues, implying that the loci of these mutants might control specific processes for the specification or neurite formation of the granule cells.

Table 3
Cerebellar mutants.

Genetic Loci	Alleles	Cerebellar Phenotypes	Other phenotypes
Group A: Early patterning mutants			
pax2a	*rk9*	Defects in MHB formation	
Group B: Mutants affecting both Purkinje and granule cells			
evanescence(eva)	*rk10*	Loss or strong reduction of granule cells; reduction of Purkinje cells	Eye degeneration
corsair(csa)	*rk11*	Loss or strong reduction of granule cells; slight reduction of Purkinje cells	
asynergy(asy)	*rk12, rk13*	Loss or strong reduction of granule cells; reduction of Purkinje cells and their dendrites	Small head; dorsally curled tail
drunken sailor(drs)	*rk14*	Loss or strong reduction of granule cells; reduction of Purkinje cells and their dendrites	Small head; dorsally curled tail
zuwai(zuw)	*rk15*	Loss or strong reduction of granule cells; reduction of Purkinje cells and their dendrites	Small head
Group C: Mutants affecting Purkinje/granule cells and showing severe abnormalities in other tissues			
gauri(gau)	*rk16*	Loss or strong reduction of granule cells; reduction of Purkinje cells in medial regions	Small head; abnormal cranial muscle
Group D: Mutants affecting granule cells only			
gazami(gaz)	*rk17*	Loss of granule cells	
Group E: Mutants affecting neurite formation			
shiomaneki(sio)	*rk18*	Parallel fibers to CC are short	

MHB, mid-hindbrain boundary.

Discussion

Conserved and non-conserved gene expression profiles in the zebrafish cerebellum

Using molecular markers, we described the individual cell types of the adult zebrafish cerebellum (Figs. 2, 3, Table 1). Although there are some structural differences between the mammalian and the zebrafish cerebellum, the expression profile of GABAergic and glutamatergic neurons in the zebrafish cerebellum is similar to that reported for mammals. These similarities indicated that the mammalian and zebrafish cerebellum use the same molecular machinery in their functions and probably in their development. Thus, studies of zebrafish cerebellum could lead to a better understanding of the function, development, and abnormalities of the mammalian cerebellum. We also found, however, some differences in the gene expression profiles between the mammalian and zebrafish cerebellum. Parvalbumin is expressed not only in Purkinje cells but also in other GABAergic interneurons in the mammalian cerebellum (Celio, 1990; Celio and Heizmann, 1981), whereas *parvalbumin7* is specifically expressed in Purkinje cells in the zebrafish. It is possible that other parvalbumin gene(s) are expressed in non-Purkinje GABAergic neurons in the zebrafish. This is unlikely, however, since an anti-Parvalbumin antibody that is reported to recognize Purkinje cells and other GABAergic neurons in mammals only detected Purkinje cells in zebrafish, as did an anti-Pvalb7 antibody (data not shown), suggesting that species-specific changes also occurred during evolution.

Zebrin II/*aldolase C* shows compartment-specific expression in the mammalian cerebellum, but neither zebrin II staining nor *aldocl* expression shows parasagittal compartmentalization in the zebrafish or other teleost species (Brochu et al., 1990; Lannoo et al., 1991a,b; Meek et al., 1992) (Fig. 2). This raises two possibilities; either (1) there are zebrin II-negative Purkinje cells but the zebrin II-positive and negative Purkinje cells do not show compartmentalization, or (2) there is no compartmentalization that is detectable by the expression of zebrin II/*aldocl* expression. In zebrafish cerebellum, the anti-zebrin II antibody stained the same population of Purkinje cells as the anti-Pvalb7 (also anti-pan Pvalb), anti-Ca8, and M1 antibodies (Fig. 2) (Miyamura and Nakayasu, 2001). Pvalb and Ca8 are expressed in all the Purkinje cells of the mammalian cerebellum (Celio, 1990; Celio and Heizmann, 1981; Hirota et al., 2003; Kato, 1990; Nogradi et al., 1997). These data indicate that Pvalb7, Ca8, and zebrin II-expressing Purkinje cells are the sole Purkinje cells in the zebrafish cerebellum. The compartmentalized expression of zebrin II in mammals is proposed to be related to the functional compartmentalization of Purkinje cells, because it correlates with the parasagittal expression of other functional molecules and the compartmentalized innervations of afferent/efferent fibers (Croci et al., 2006; Larouche and Hawkes, 2006; Voogd et al., 2003). The uniform expression of zebrin II and the other markers for Purkinje cells in zebrafish may reflect a greater simplicity in their function in the fish cerebellum.

Cerebellum-like structures

The valvula cerebelli (Va), corpus cerebella (CCe), and vestibulolateral lobe (EG and LCa) are major parts of the teleost cerebellum. In addition, the EG-CC-MON circuitry in the hindbrain, and the TL-SM-Type I neuron circuitry in the midbrain are proposed to display similar structures and functions to the cerebellum in most teleost species, and they, with the cerebellum, are called cerebellum-like structures (Bell, 2002; Bell et al., 2008; Mikami et al., 2004). All these structures contain Purkinje-like cells that receive inputs from parallel fibers. We found that *pvalb7* was expressed in the Purkinje-like crest cells in the MON that extended Pvalb7$^+$ dendrites into the CC (Figs. 2, 8), and that the dendrites of crest cells received inputs from Vglut1$^+$ parallel fibers of the EG (Fig. 11). Similarly, the Pvalb7$^+$ dendrites of type I neurons received inputs from Vglut1$^+$ parallel fibers originating from granule-like cells of the torus longitudinalis (TL, Fig. 11). These findings indicate that the cerebellum-like structures, both the EG-CC-MON and TL-SM-Type I neuron circuitries, utilize Pvalb7 and Vglut1 for their function. *gad1*$^+$ cells were also detected in the CC, as in the ML of the Va and CCe of the cerebellum (Fig. 2), and are presumably stellate-like GABAergic interneurons. Thus, these cerebellum-like structures use at least some molecules used by the cerebellum to function. In contrast, we found that *ca8* and *zebrin II (aldocl)* are specifically expressed in Purkinje cells but not Purkinje-like cells (crest cells and type I neurons). The difference in the gene expression profiles between Purkinje and other Purkinje-like cells may reflect differences in their developmental origins (VZ of rhombomere 1 versus that of the medial hindbrain and midbrain) or in their function; i.e., Purkinje but not Purkinje-like cells receive strong synaptic inputs from a single presynaptic climbing fiber (Bell, 2002; Meek and Nieuwenhuys, 1991).

Compartmentalization of granule cells

In the adult zebrafish cerebellum, the granule cells are located underneath the Purkinje cell layer, but they were superficial in the EG and LCa (Altman and Bayer, 1997; Butler and Hodos, 1996; Wullimann et al., 1996). Parallel fibers from the EG but not from the CCe innervate the dendrites of the crest cells in the CC (Montgomery, 1981; Puzdrowski, 1989; Volkmann et al., 2008). The granule cells of the CCe, EG, and LCa are reported to migrate along different paths to their final destination (Volkmann et al., 2008). These findings suggest differences among the functions and developmental processes of the Va, CCe, EG, and LCa. In this study, we found two differences in development and gene expression profiles between the granule cells in the Va, CCe and EG, and those in the LCa. First, we found that granule cells start to differentiate at around 3 to 3.5 dpf in the EG and CCe (possibly Va), and that those in the LCa differentiated later (Fig. 13). Second, we could distinguish granule cells in the Va/CCe/EG and LCa of the adult cerebellum by the expression of certain genetic markers (Fig. 3, Suppl. Fig. 2, and Table 1). Although the granule cells of the Va/CCe/EG and LCa may be derived from the URL and similarly extend parallel fibers, they may undergo slightly different developmental processes. The different gene expression profiles of these two populations probably reflect functional differences. Future studies will shed light on the genetic programs that distinguish the development and functions of these granule cells.

Efferent tracts: eurydendroid cells and cerebellovestibular tracts

Eurydendroid cells are a teleost-specific cell population that receives inputs from the axons of Purkinje cells and corresponds to the DCN of the mammalian cerebellum (Butler and Hodos, 1996; Ikenaga et al., 2005, 2006). As previously reported (Alonso et al., 1992; Porteros et al., 1998), we found that Pvalb7$^-$ somata receive inputs from the Pvalb7$^+$ axons of Purkinje cells (Fig. 2). These cells should be eurydendroid cells in the zebrafish. We further found that some, if not all, of these eurydendroid cells express high levels of *vglut2a/b* (Fig. 3), indicating that some of the *vglut2*^{high} cells are eurydendroid cells. During the development of the mouse cerebellum, while both *Vglut1* and *Vglut2* are expressed in granule cells, *Vglut1* and *Vglut2* show preferential expression in mature and immature granule cells, respectively (Miyazaki et al., 2003). From the early postnatal stage to adulthood, *Vglut1* is expressed in granule cells, and *Vglut2* is preferentially expressed in the DCN (Miyazaki et al., 2003). Therefore, the expression of *vglut1* in the granule cells and of *vglut2a/b* in eurydendroid cells of the adult cerebellum is conserved among vertebrate species, further supporting the concept that eurydendroid cells are equivalent to the DCN of the mammalian cerebellum.

olig2$^+$ neurons were recently reported to be located in the vicinity of the PCL in zebrafish and to have eurydendroid-like neurites

(McFarland et al., 2008). We confirmed that the *olig2*$^+$ neurons have long neurites (EGFP$^+$ neurites in the *Tg(olig2:EGFP)* line) that extend to the ML and GCL of the adult cerebellum (Fig. 5). The neurites of *olig2*$^+$ neurons resemble those of eurydendroid cells, which send their axons outside of the cerebellum and their dendrites into the ML (Ikenaga et al., 2005, 2006). However, these neurons did not stain with an anti-calretinin antibody (McFarland et al., 2008) (Suppl. Fig. 3), which recognizes eurydendroid cells (Castro et al., 2006; Diaz-Regueira and Anadon, 2000; Meek et al., 2008) (Fig. 7), implying that the *olig2*$^+$ neurons are different from CR-ir$^+$ eurydendroid cells. We detected *olig2*$^+$ cells near the PCL as well as in the deep GCL and VZ in the adult cerebellum, and also found that some of the *olig2*$^+$ cells could incorporate BrdU (Fig. 5). Our data indicate that *olig2* is expressed in both neural progenitors (VZ), and undifferentiated (deep GCL) and differentiated neurons (beneath the PCL), in addition to oligodendrocytes, in the adult cerebellum. Our findings also suggest that the *olig2*$^+$ neurons are derived from the VZ. As in mice, neural progenitors in the zebrafish VZ express the proneural gene *ptf1a* (Lin et al., 2004; Zecchin et al., 2004), which is known to play an essential role in the development of GABAergic neurons (Hoshino, 2006; Hoshino et al., 2005). We found that a portion of *olig2*$^+$ cells also express *ptf1a* in the VZ of the cerebellum (unpublished results). However, the *olig2*$^+$ neurons do not express *gad1*, *gad2*, *glyt1*, or *glyt2* (McFarland et al., 2008) (Fig. 5, data not shown for *glyt1/2*). Instead, we found that at least some of the *olig2*$^+$ neurons express *vglut2a* and receive inputs from Purkinje cell axons, like eurydendroid cells (Fig. 5). These findings suggest that, although the *olig2*$^+$ neurons are from the VZ, they function as eurydendroid cells.

There are both glutamatergic and GABAergic neurons in the DCN of the mammalian cerebellum (Hoshino, 2006), whereas GABAergic eurydendroid cells have not been identified (Ikenaga et al., 2005). In zebrafish, axons from calretinin-immunoreactive (CR-ir$^+$), *vglut2*^{high} neurons and *olig2*$^+$, CR-ir$^-$, *vglut2*^{high} neurons (the eurydendroid cells) may compose the glutamatergic efferent tracts that convey information from the Purkinje and parallel fibers to other regions of the brain.

CR-ir$^-$ and CR-ir$^+$ eurydendroid cells are also reported for the mormyrid fish (Meek et al., 2008). The presence of these two eurydendroid cells is likely a common feature among teleost species.

Most of the output information is conveyed by eurydendroid cells from the teleost cerebellum (Butler and Hodos, 1996). Immunostaining of the Purkinje cell axons with anti-Pvalb7 and anti-zebrin II, and tracing experiments revealed that the presence of direct efferent tracts from the Purkinje cells in the lateral region of the CCe to the vestibular regions (Fig. 8). Although the cerebellovestibular tracts are reported in amphibians (Gonzalez et al., 1984; Llinas et al., 1967), it has not been well characterized in teleosts. The cerebellovestibular tracts are involved in precise motor controls, such as the vestibulo-ocular reflex (Ito, 2002a, 2006). Our data suggest that the direct efferent tracts from the Purkinje cells to the vestibular region are conserved among vertebrate species.

Bergmann glia

We characterized the Bergmann glial cells by their expression of Blbp (Fabp7a, Fig. 4). Blbp$^+$ (also Gfap$^+$) Bergmann glial cells are distributed homogeneously throughout the mammalian cerebellum (Arnold et al., 1994; de Blas, 1984; de Blas and Cherwinski, 1985; Feng and Heintz, 1995; Rousselot et al., 1997). We found that Blbp$^+$ cells are localized more heavily to the antero-medial region than to the lateral regions of the zebrafish cerebellum (Fig. 4). The Blbp$^+$ radial glial cells are known to serve as neural precursors in the mammalian telencephalon (Hartfuss et al., 2001; Malatesta et al., 2003, 2000; Pinto and Gotz, 2007). It was recently reported that some of the Blbp$^+$ Bergmann glial cells proliferate in the cerebellum of the adult rabbit (Ponti et al., 2008). These findings suggest that the Blbp$^+$ Bergmann glial cells may also function as neural precursors in the zebrafish adult cerebellum. Proliferating cells are located in the anterior and medial regions of the ML in the adult zebrafish cerebellum (Zupanc et al., 2005), as are the Blbp$^+$ Bergmann glial cells. Future analysis of the proliferation status of the Bergmann glial cells will clarify this point.

Bergmann glial cells are known to function as glutamate scavengers (Bellamy, 2006). We found that Blbp$^+$ Bergmann glial cells express an astrocyte-specific glutamate transporter gene, *glastb (slc1a3b)* (Fig. 4), further demonstrating the functional conservation of Bergmann glia between mammals and teleosts.

Conserved afferent tracts

ptf1a and *pou4f1 (brn3a)* are expressed in the IO of zebrafish larvae and adults (Fig. 6), as in mice (Fedtsova and Turner, 1995; Yamada et al., 2007). The EGFP signals in the *Tg(pou4f1-hsp70l:EGFP)* line enabled us to trace the climbing fibers (Fig. 6). We found that the climbing fibers terminate on the soma or proximal dendrites of Purkinje cells in zebrafish (Fig. 6) and that they are Vglut2a$^+$ glutamatergic, as in other vertebrate species (Altman and Bayer, 1997; Bell, 2002, 2008; Hisano et al., 2002; Miyazaki et al., 2003). Thus, the climbing fibers are highly conserved among vertebrate species. In this study, we were unable to dissect the mossy fibers except for the zn5$^+$ mossy fibers from the dorsal tegmental nuclei (Fig. 7) and the Vglut2a$^+$ presynaptic boutons of mossy fibers in the cerebellar glomeruli (Fig. 9). The neurons of pre-cerebellar nuclei other than the IO are derived from the *atoh1* (*Math1*)-expressing neural progenitors located in the murine and avian rhombic lip (RL) (Machold and Fishell, 2005; Wang et al., 2005; Wilson and Wingate, 2006; Wingate, 2005). Lineage tracing of the neural progenitors expressing *atoh1*-family genes may clarify the origin of the *alcam*$^+$ (zn5$^+$) mossy fiber neurons and the identities of the neurons in the other pre-cerebellar nuclei.

Genetic studies of cerebellar development

In the zebrafish, the differentiation of granule and Purkinje cells begins around 3 dpf (Fig. 12). The *vglut1*$^+$ granule cells are located beneath the Pvalb7$^+$ Purkinje cells in the prospective CCe region, and the Purkinje cells extend their dendrites and received inputs from the parallel fibers of the granule cells at 5 dpf (Fig. 6). These data indicate that a simple layer structure forms by 5 dpf, and led us to screen for mutations affecting the development of the cerebellar neurons and neural circuits in the first week (Fig. 13, Table 3). Previously, morphology-based screening of mutations affecting cerebellar formation identified genes involved in early neural patterning (Brand et al., 1996; Schier et al., 1996) (group A mutants in our screening), but did not isolate mutations affecting the development of individual cerebellar neurons and their circuits.

Using anti-Pvalb7 and anti-Vglut1 antibodies, we were able to isolate mutations affecting the development and maintenance of Purkinje and granule cells, and the neural circuits involving these neurons. Group B and C mutants (Table 3) showed a reduction or loss of both Purkinje and granule cells but did not show abnormalities in the formation of the midbrain–hindbrain boundary (MHB). These mutant loci may encode molecules involved in the maintenance of cerebellar neurons or in particular developmental processes that are shared by both Purkinje and granule cells. They may include genes responsible for genetic disorders of cerebellar development and function, such as spinocerebellar ataxia (Koeppen, 2005). These genes may also control other developmental processes, since some of the mutants, such as *eva*, *asy*, and *drs*, also showed specific phenotypes in other tissues.

The *gaz* mutant embryos in group D showed specific defects in the development of granule cells, while the development of Purkinje cells

was grossly normal, suggesting that the absence of granule cells does not affect the differentiation of Purkinje cells. Precise analyses of the mutants should clarify whether the formation of Purkinje cell dendrites and presynaptic sites depends on the formation of parallel fibers. *sio* in group E affected the formation of parallel fibers to the CC, and this mutant locus may function in axogenesis or in the determination of posterior granule cells that extend the parallel fibers to the CC.

Further analyses of these mutants with molecular markers and transgenic lines will reveal the roles of the mutant loci in the development of cerebellar neurons and their neurites. In addition, the identification of the loci will clarify which genetic cascades control cerebellar development.

In summary, we described the anatomy of the cerebellar neurons and neural circuits of the zebrafish cerebellum using molecular markers. Along with our isolation of cerebellar mutants, our data provide a platform for studying the development and functions of the zebrafish cerebellum as a model system for vertebrate higher brain structure.

Acknowledgments

We thank B. Appel for the *Tg(olig2:EGFP)vu12* line and anti-Sox10 antibody; S.D. Leach for the *Tg(ptf1a:eGFP)jh1* line; H. Okamoto for the *Tg(pou4f1-hsp70l:EGFP)rw0110b* line; R. Hawkes for the anti-zebrin II antibody; W. S. Talbot for anti-Mbp antibody; the Zebrafish International Resource Center (ZIRC, supported by grant P40 RR012546 from NIH-NCRR); Y. Wataoka, Y. Kota, S. Fujii, K. Bando, and A. Katsuyama for technical assistance; and the members of the Hibi Laboratory for helpful discussions. This work was supported by a grant from NCC, Korea (NCC 0810060-1 to Y.-K., B) and by a grant from RIKEN (to M.H.).

Appendix A. Supplementary data

Supplementary data associated with this article can be found, in the online version, at doi:10.1016/j.ydbio.2009.04.013.

References

Adolf, B., Chapouton, P., Lam, C.S., Topp, S., Tannhauser, B., Strahle, U., Gotz, M., Bally-Cuif, L., 2006. Conserved and acquired features of adult neurogenesis in the zebrafish telencephalon. Dev. Biol. 295, 278–293.

Ahn, A.H., Dziennis, S., Hawkes, R., Herrup, K., 1994. The cloning of zebrin II reveals its identity with aldolase C. Development 120, 2081–2090.

Aizawa, H., Bianco, I.H., Hamaoka, T., Miyashita, T., Uemura, O., Concha, M.L., Russell, C., Wilson, S.W., Okamoto, H., 2005. Laterotopic representation of left–right information onto the dorso-ventral axis of a zebrafish midbrain target nucleus. Curr. Biol. 15, 238–243.

Alder, J., Cho, N.K., Hatten, M.E., 1996. Embryonic precursor cells from the rhombic lip are specified to a cerebellar granule neuron identity. Neuron 17, 389–399.

Alonso, J.R., Arevalo, R., Brinon, J.G., Lara, J., Weruaga, E., Aijon, J., 1992. Parvalbumin immunoreactive neurons and fibres in the teleost cerebellum. Anat. Embryol. (Berl). 185, 355–361.

Altman, J., Bayer, S.A., 1997. Development of the cerebellar system in relation to its evolution, structure, and function. CRC Press, Inc., Boca Raton, FL.

Arnold, D., Feng, L., Kim, J., Heintz, N., 1994. A strategy for the analysis of gene expression during neural development. Proc. Natl. Acad. Sci. U. S. A. 91, 9970–9974.

Aruga, J., Yokota, N., Hashimoto, M., Furuichi, T., Fukuda, M., Mikoshiba, K., 1994. A novel zinc finger protein, zic, is involved in neurogenesis, especially in the cell lineage of cerebellar granule cells. J. Neurochem. 63, 1880–1890.

Bell, C.C., 2002. Evolution of cerebellum-like structures. Brain Behav. Evol. 59, 312–326.

Bell, C.C., Han, V., Sawtell, N.B., 2008. Cerebellum-like structures and their implications for cerebellar function. Annu. Rev. Neurosci. 31, 1–24.

Bellamy, T.C., 2006. Interactions between Purkinje neurones and Bergmann glia. Cerebellum 5, 116–126.

Belting, H.G., Hauptmann, G., Meyer, D., Abdelilah-Seyfried, S., Chitnis, A., Eschbach, C., Soll, I., Thisse, C., Thisse, B., Artinger, K.B., Lunde, K., Driever, W., 2001. spiel ohne grenzen/pou2 is required during establishment of the zebrafish midbrain–hindbrain boundary organizer. Development 128, 4165–4176.

Ben-Arie, N., Bellen, H.J., Armstrong, D.L., McCall, A.E., Gordadze, P.R., Guo, Q., Matzuk, M.M., Zoghbi, H.Y., 1997. Math1 is essential for genesis of cerebellar granule neurons. Nature 390, 169–172.

Boulland, J.L., Qureshi, T., Seal, R.P., Rafiki, A., Gundersen, V., Bergersen, L.H., Fremeau Jr., R.T., Edwards, R.H., Storm-Mathisen, J., Chaudhry, F.A., 2004. Expression of the vesicular glutamate transporters during development indicates the widespread corelease of multiple neurotransmitters. J. Comp. Neurol. 480, 264–280.

Brand, M., Heisenberg, C.P., Jiang, Y.J., Beuchle, D., Lun, K., Furutani-Seiki, M., Granato, M., Haffter, P., Hammerschmidt, M., Kane, D.A., Kelsh, R.N., Mullins, M.C., Odenthal, J., van Eeden, F.J., Nusslein-Volhard, C., 1996. Mutations in zebrafish genes affecting the formation of the boundary between midbrain and hindbrain. Development 123, 179–190.

Brochu, G., Maler, L., Hawkes, R., 1990. Zebrin II: a polypeptide antigen expressed selectively by Purkinje cells reveals compartments in rat and fish cerebellum. J. Comp. Neurol. 291, 538–552.

Brosamle, C., Halpern, M.E., 2002. Characterization of myelination in the developing zebrafish. Glia 39, 47–57.

Bruce, A.E., Howley, C., Zhou, Y., Vickers, S.L., Silver, L.M., King, M.L., Ho, R.K., 2003. The maternally expressed zebrafish T-box gene eomesodermin regulates organizer formation. Development 130, 5503–5517.

Buckles, G.R., Thorpe, C.J., Ramel, M.C., Lekven, A.C., 2004. Combinatorial Wnt control of zebrafish midbrain–hindbrain boundary formation. Mech. Dev. 121, 437–447.

Butler, A.B., Hodos, H., 1996. Comparative Vertebrate Neuroanatomy: Evolution and Adaptation. Wiley-Liss, New York.

Castejon, O.J., 1990. Surface and membrane morphology of Bergmann glial cells and their topographic relationships in the cerebellar molecular layer. J. Submicrosc. Cytol. Pathol. 22, 123–134.

Castejon, O.J., Castejon, H.V., Sims, P., 2000. Confocal, scanning and transmission electron microscopic study of cerebellar mossy fiber glomeruli. J. Submicrosc. Cytol. Pathol. 32, 247–260.

Castro, A., Becerra, M., Manso, M.J., Anadon, R., 2006. Calretinin immunoreactivity in the brain of the zebrafish, *Danio rerio*: distribution and comparison with some neuropeptides and neurotransmitter-synthesizing enzymes. II. Midbrain, hindbrain, and rostral spinal cord. J. Comp. Neurol. 494, 792–814.

Celio, M.R., 1990. Calbindin D-28k and parvalbumin in the rat nervous system. Neuroscience 35, 375–475.

Celio, M.R., Heizmann, C.W., 1981. Calcium-binding protein parvalbumin as a neuronal marker. Nature 293, 300–302.

Colombo, A., Reig, G., Mione, M., Concha, M.L., 2006. Zebrafish BarH-like genes define discrete neural domains in the early embryo. Gene Expression Patterns 6, 347–352.

Costagli, A., Kapsimali, M., Wilson, S.W., Mione, M., 2002. Conserved and divergent patterns of Reelin expression in the zebrafish central nervous system. J. Comp. Neurol. 450, 73–93.

Crespo, C., Porteros, A., Arevalo, R., Brinon, J.G., Aijon, J., Alonso, J.R., 1999. Distribution of parvalbumin immunoreactivity in the brain of the tench (*Tinca tinca* L., 1758). J. Comp. Neurol. 413, 549–571.

Croci, L., Chung, S.H., Masserdotti, G., Gianola, S., Bizzoca, A., Gennarini, G., Corradi, A., Rossi, F., Hawkes, R., Consalez, G.G., 2006. A key role for the HLH transcription factor EBF2COE2,O/E-3 in Purkinje neuron migration and cerebellar cortical topography. Development 133, 2719–2729.

de Blas, A.L., 1984. Monoclonal antibodies to specific astroglial and neuronal antigens reveal the cytoarchitecture of the Bergmann glia fibers in the cerebellum. J. Neurosci. 4, 265–273.

de Blas, A.L., Cherwinski, H.M., 1985. The development of the Bergmann fiber palisades in the cerebellum of the normal rat and in the weaver mouse. Brain Res. 342, 234–241.

Diaz-Regueira, S., Anadon, R., 2000. Calretinin expression in specific neuronal systems in the brain of an advanced teleost, the grey mullet (*Chelon labrosus*). J. Comp. Neurol. 426, 81–105.

Driever, W., Solnica-Krezel, L., Schier, A.F., Neuhauss, S.C., Malicki, J., Stemple, D.L., Stainier, D.Y., Zwartkruis, F., Abdelilah, S., Rangini, Z., Belak, J., Boggs, C., 1996. A genetic screen for mutations affecting embryogenesis in zebrafish. Development 123, 37–46.

Fedtsova, N.G., Turner, E.E., 1995. Brn-3.0 expression identifies early post-mitotic CNS neurons and sensory neural precursors. Mech. Dev. 53, 291–304.

Feng, L., Heintz, N., 1995. Differentiating neurons activate transcription of the brain lipid-binding protein gene in radial glia through a novel regulatory element. Development 121, 1719–1730.

Folgueira, M., Anadon, R., Yanez, J., 2006. Afferent and efferent connections of the cerebellum of a salmonid, the rainbow trout (*Oncorhynchus mykiss*): a tract-tracing study. J. Comp. Neurol. 497, 542–565.

Foucher, I., Mione, M., Simeone, A., Acampora, D., Bally-Cuif, L., Houart, C., 2006. Differentiation of cerebellar cell identities in absence of Fgf signalling in zebrafish Otx morphants. Development 133, 1891–1900.

Godinho, L., Williams, P.R., Claassen, Y., Provost, E., Leach, S.D., Kamermans, M., Wong, R.O., 2007. Nonapical symmetric divisions underlie horizontal cell layer formation in the developing retina in vivo. Neuron 56, 597–603.

Gonzalez, A., ten Donkelaar, H.J., de Boer-van Huizen, R., 1984. Cerebellar connections in *Xenopus laevis*. An HRP study. Anat. Embryol. (Berl) 169, 167–176.

Gravel, C., Hawkes, R., 1990. Parasagittal organization of the rat cerebellar cortex: direct comparison of Purkinje cell compartments and the organization of the spinocerebellar projection. J. Comp. Neurol. 291, 79–102.

Haffter, P., Granato, M., Brand, M., Mullins, M.C., Hammerschmidt, M., Kane, D.A., Odenthal, J., van Eeden, F.J., Jiang, Y.J., Heisenberg, C.P., Kelsh, R.N., Furutani-Seiki, M., Vogelsang, E., Beuchle, D., Schach, U., Fabian, C., Nusslein-Volhard, C., 1996. The identification of genes with unique and essential functions in the development of the zebrafish, *Danio rerio*. Development 123, 1–36.

Hartfuss, E., Galli, R., Heins, N., Gotz, M., 2001. Characterization of CNS precursor subtypes and radial glia. Dev. Biol. 229, 15–30.

Higashijima, S., Mandel, G., Fetcho, J.R., 2004a. Distribution of prospective glutamatergic,

glycinergic, and GABAergic neurons in embryonic and larval zebrafish. J. Comp. Neurol. 480, 1–18.
Higashijima, S., Schaefer, M., Fetcho, J.R., 2004b. Neurotransmitter properties of spinal interneurons in embryonic and larval zebrafish. J. Comp. Neurol. 480, 19–37.
Hirota, J., Ando, H., Hamada, K., Mikoshiba, K., 2003. Carbonic anhydrase-related protein is a novel binding protein for inositol 1,4,5-trisphosphate receptor type 1. Biochem. J. 372, 435–441.
Hisano, S., Sawada, K., Kawano, M., Kanemoto, M., Xiong, G., Mogi, K., Sakata-Haga, H., Takeda, J., Fukui, Y., Nogami, H., 2002. Expression of inorganic phosphate/vesicular glutamate transporters (BNPI/VGLUT1 and DNPI/VGLUT2) in the cerebellum and precerebellar nuclei of the rat. Brain Res. Mol. Brain Res. 107, 23–31.
Horikawa, K., Ishimatsu, K., Yoshimoto, E., Kondo, S., Takeda, H., 2006. Noise-resistant and synchronized oscillation of the segmentation clock. Nature 441, 719–723.
Hoshino, M., 2006. Molecular machinery governing GABAergic neuron specification in the cerebellum. Cerebellum 5, 193–198.
Hoshino, M., Nakamura, S., Mori, K., Kawauchi, T., Terao, M., Nishimura, Y.V., Fukuda, A., Fuse, T., Matsuo, N., Sone, M., Watanabe, M., Bito, H., Terashima, T., Wright, C.V., Kawaguchi, Y., Nakao, K., Nabeshima, Y., 2005. Ptf1a, a bHLH transcriptional gene, defines GABAergic neuronal fates in cerebellum. Neuron 47, 201–213.
Ikenaga, T., Yoshida, M., Uematsu, K., 2005. Morphology and immunohistochemistry of efferent neurons of the goldfish corpus cerebelli. J. Comp. Neurol. 487, 300–311.
Ikenaga, T., Yoshida, M., Uematsu, K., 2006. Cerebellar efferent neurons in teleost fish. Cerebellum 5, 268–274.
Ito, M., 2002a. Historical review of the significance of the cerebellum and the role of Purkinje cells in motor learning. Ann. N. Y. Acad. Sci. 978, 273–288.
Ito, M., 2002b. The molecular organization of cerebellar long-term depression. Nat. Rev. Neurosci. 3, 896–902.
Ito, M., 2006. Cerebellar circuitry as a neuronal machine. Prog. Neurobiol. 78, 272–303.
Ito, M., 2008. Control of mental activities by internal models in the cerebellum. Nat. Rev. Neurosci. 9, 304–313.
Jande, S.S., Tolnai, S., Lawson, D.E., 1981. Immunohistochemical localization of vitamin D-dependent calcium-binding protein in duodenum, kidney, uterus and cerebellum of chickens. Histochemistry 71, 99–116.
Jaszai, J., Reifers, F., Picker, A., Langenberg, T., Brand, M., 2003. Isthmus-to-midbrain transformation in the absence of midbrain–hindbrain organizer activity. Development 130, 6611–6623.
Jowett, T., Yan, Y.L., 1996. Double fluorescent in situ hybridization to zebrafish embryos. Trends Genet. 12, 387–389.
Kanki, J.P., Chang, S., Kuwada, J.Y., 1994. The molecular cloning and characterization of potential chick DM-GRASP homologs in zebrafish and mouse. J. Neurobiol. 25, 831–845.
Kato, K., 1990. Sequence of a novel carbonic anhydrase-related polypeptide and its exclusive presence in Purkinje cells. FEBS Lett. 271, 137–140.
Kikuchi, Y., Segawa, H., Tokumoto, M., Tsubokawa, T., Hotta, Y., Uyemura, K., Okamoto, H., 1997. Ocular and cerebellar defects in zebrafish induced by overexpression of the LIM domains of the islet-3 LIM/homeodomain protein. Neuron 18, 369–382.
Kimura, Y., Okamura, Y., Higashijima, S., 2006. alx, a zebrafish homolog of Chx10, marks ipsilateral descending excitatory interneurons that participate in the regulation of spinal locomotor circuits. J. Neurosci. 26, 5684–5697.
Koeppen, A.H., 2005. The pathogenesis of spinocerebellar ataxia. Cerebellum 4, 62–73.
Koster, R.W., Fraser, S.E., 2001. Direct imaging of in vivo neuronal migration in the developing cerebellum. Curr. Biol. 11, 1858–1863.
Lannoo, M.J., Brochu, G., Maler, L., Hawkes, R., 1991a. Zebrin II immunoreactivity in the rat and in the weakly electric teleost Eigenmannia (gymnotiformes) reveals three modes of Purkinje cell development. J. Comp. Neurol. 310, 215–233.
Lannoo, M.J., Ross, L., Maler, L., Hawkes, R., 1991b. Development of the cerebellum and its extracerebellar Purkinje cell projection in teleost fishes as determined by zebrin II immunocytochemistry. Prog. Neurobiol. 37, 329–363.
Larouche, M., Hawkes, R., 2006. From clusters to stripes: the developmental origins of adult cerebellar compartmentation. Cerebellum 5, 77–88.
Lin, J.W., Biankin, A.V., Horb, M.E., Ghosh, B., Prasad, N.B., Yee, N.S., Pack, M.A., Leach, S.D., 2004. Differential requirement for ptf1a in endocrine and exocrine lineages of developing zebrafish pancreas. Dev. Biol. 270, 474–486.
Llinas, R., Precht, W., Kitai, S.T., 1967. Cerebellar Purkinje cell projection to the peripheral vestibular organ in the frog. Science 158, 1328–1330.
Lyons, D.A., Pogoda, H.M., Voas, M.G., Woods, I.G., Diamond, B., Nix, R., Arana, N., Jacobs, J., Talbot, W.S., 2005. erbb3 and erbb2 are essential for Schwann cell migration and myelination in zebrafish. Curr. Biol. 15, 513–524.
Machold, R., Fishell, G., 2005. Math1 is expressed in temporally discrete pools of cerebellar rhombic-lip neural progenitors. Neuron 48, 17–24.
Malatesta, P., Hack, M.A., Hartfuss, E., Kettenmann, H., Klinkert, W., Kirchhoff, F., Gotz, M., 2003. Neuronal or glial progeny: regional differences in radial glia fate. Neuron 37, 751–764.
Malatesta, P., Hartfuss, E., Gotz, M., 2000. Isolation of radial glial cells by fluorescent-activated cell sorting reveals a neuronal lineage. Development 127, 5253–5263.
Martin, S.C., Heinrich, G., Sandell, J.H., 1998. Sequence and expression of glutamic acid decarboxylase isoforms in the developing zebrafish. J. Comp. Neurol. 396, 253–266.
Martyniuk, C.J., Awad, R., Hurley, R., Finger, T.E., Trudeau, V.L., 2007. Glutamic acid decarboxylase 65, 67, and GABA-transaminase mRNA expression and total enzyme activity in the goldfish (*Carassius auratus*) brain. Brain Res. 1147, 154–166.
McFarland, K.A., Topczewska, J.M., Weidinger, G., Dorsky, R.I., Appel, B., 2008. Hh and Wnt signaling regulate formation of olig2+ neurons in the zebrafish cerebellum. Dev. Biol. 318, 162–171.
Meek, J., Hafmans, T.G., Maler, L., Hawkes, R., 1992. Distribution of zebrin II in the gigantocerebellum of the mormyrid fish *Gnathonemus petersii* compared with other teleosts. J. Comp. Neurol. 316, 17–31.
Meek, J., Nieuwenhuys, R., 1991. Palisade pattern of mormyrid Purkinje cells: a correlated light and electron microscopic study. J. Comp. Neurol. 306, 156–192.
Meek, J., Schellart, N.A., 1978. A Golgi study of goldfish optic tectum. J. Comp. Neurol. 182, 89–122.
Meek, J., Yang, J.Y., Han, V.Z., Bell, C.C., 2008. Morphological analysis of the mormyrid cerebellum using immunohistochemistry, with emphasis on the unusual neuronal organization of the valvula. J. Comp. Neurol. 510, 396–421.
Mikami, Y., Yoshida, T., Matsuda, N., Mishina, M., 2004. Expression of zebrafish glutamate receptor delta2 in neurons with cerebellum-like wiring. Biochem. Biophys. Res. Commun. 322, 168–176.
Miyamura, Y., Nakayasu, H., 2001. Zonal distribution of Purkinje cells in the zebrafish cerebellum: analysis by means of a specific monoclonal antibody. Cell Tissue Res. 305, 299–305.
Miyazaki, T., Fukaya, M., Shimizu, H., Watanabe, M., 2003. Subtype switching of vesicular glutamate transporters at parallel fibre-Purkinje cell synapses in developing mouse cerebellum. Eur. J. Neurosci. 17, 2563–2572.
Montgomery, J.C., 1981. Origin of the parallel fibers in the cerebellar crest overlying the intermediate nucleus of the elasmobranch hindbrain. J. Comp. Neurol. 202, 185–191.
Mueller, T., Wullimann, M.F., 2005. Atlas of Early Zebrafish Brain Development: A Tool for Molecular Neurogenetics. Elsevier B. V., The Netherlands.
Murakami, T., Morita, Y., 1987. Morphology and distribution of the projection neurons in the cerebellum in a teleost, *Sebastiscus marmoratus*. J. Comp. Neurol. 256, 607–623.
Nogradi, A., Jonsson, N., Walker, R., Caddy, K., Carter, N., Kelly, C., 1997. Carbonic anhydrase II and carbonic anhydrase-related protein in the cerebellar cortex of normal and lurcher mice. Brain Res. Dev. Brain Res. 98, 91–101.
Park, H.C., Boyce, J., Shin, J., Appel, B., 2005. Oligodendrocyte specification in zebrafish requires notch-regulated cyclin-dependent kinase inhibitor function. J. Neurosci. 25, 6836–6844.
Park, H.C., Mehta, A., Richardson, J.S., Appel, B., 2002. olig2 is required for zebrafish primary motor neuron and oligodendrocyte development. Dev. Biol. 248, 356–368.
Park, H.C., Shin, J., Roberts, R.K., Appel, B., 2007. An olig2 reporter gene marks oligodendrocyte precursors in the postembryonic spinal cord of zebrafish. Dev. Dyn. 236, 3402–3407.
Pinto, L., Gotz, M., 2007. Radial glial cell heterogeneity—the source of diverse progeny in the CNS. Prog. Neurobiol. 83, 2–23.
Pisharath, H., Rhee, J.M., Swanson, M.A., Leach, S.D., Parsons, M.J., 2007. Targeted ablation of beta cells in the embryonic zebrafish pancreas using *E. coli* nitroreductase. Mech. Dev. 124, 218–229.
Ponti, G., Peretto, P., Bonfanti, L., 2008. Genesis of neuronal and glial progenitors in the cerebellar cortex of peripuberal and adult rabbits. PLoS ONE 3, e2366.
Porteros, A., Arevalo, R., Brinon, J.G., Crespo, C., Aijon, J., Alonso, J.R., 1998. Parvalbumin immunoreactivity during the development of the cerebellum of the rainbow trout. Brain Res. Dev. Brain Res. 109, 221–227.
Punnamoottil, B., Kikuta, H., Pezeron, G., Erceg, J., Becker, T.S., Rinkwitz, S., 2008. Enhancer detection in zebrafish permits the identification of neuronal subtypes that express Hox4 paralogs. Dev. Dyn. 237, 2195–2208.
Puzdrowski, R.L., 1989. Peripheral distribution and central projections of the lateral-line nerves in goldfish, *Carassius auratus*. Brain Behav. Evol. 34, 110–131.
Reifers, F., Bohli, H., Walsh, E.C., Crossley, P.H., Stainier, D.Y., Brand, M., 1998. Fgf8 is mutated in zebrafish acerebellar (ace) mutants and is required for maintenance of midbrain–hindbrain boundary development and somitogenesis. Development 125, 2381–2395.
Rodriguez, F., Duran, E., Gomez, A., Ocana, F.M., Alvarez, E., Jimenez-Moya, F., Broglio, C., Salas, C., 2005. Cognitive and emotional functions of the teleost fish cerebellum. Brain Res. Bull. 66, 365–370.
Rohrschneider, M.R., Elsen, G.E., Prince, V.E., 2007. Zebrafish Hoxb1a regulates multiple downstream genes including prickle1b. Dev. Biol. 309, 358–372.
Rousselot, P., Heintz, N., Nottebohm, F., 1997. Expression of brain lipid binding protein in the brain of the adult canary and its implications for adult neurogenesis. J. Comp. Neurol. 385, 415–426.
Schier, A.F., Neuhauss, S.C., Harvey, M., Malicki, J., Solnica-Krezel, L., Stainier, D.Y., Zwartkruis, F., Abdelilah, S., Stemple, D.L., Rangini, Z., Yang, H., Driever, W., 1996. Mutations affecting the development of the embryonic zebrafish brain. Development 123, 165–178.
Schuller, U., Kho, A.T., Zhao, Q., Ma, Q., Rowitch, D.H., 2006. Cerebellar 'transcriptome' reveals cell-type and stage-specific expression during postnatal development and tumorigenesis. Mol. Cell Neurosci. 33, 247–259.
Shin, J., Park, H.C., Topczewska, J.M., Mawdsley, D.J., Appel, B., 2003. Neural cell fate analysis in zebrafish using olig2 BAC transgenics. Methods Cell Sci. 25, 7–14.
Toyama, R., O'Connell, M.L., Wright, C.V., Kuehn, M.R., Dawid, I.B., 1995. Nodal induces ectopic goosecoid and lim1 expression and axis duplication in zebrafish. Development 121, 383–391.
Trevarrow, B., Marks, D.L., Kimmel, C.B., 1990. Organization of hindbrain segments in the zebrafish embryo. Neuron 4, 669–679.
Volkmann, K., Rieger, S., Babaryka, A., Koster, R.W., 2008. The zebrafish cerebellar rhombic lip is spatially patterned in producing granule cell populations of different functional compartments. Dev. Biol. 313, 167–180.
Voogd, J., Pardoe, J., Ruigrok, T.J., Apps, R., 2003. The distribution of climbing and mossy fiber collateral branches from the copula pyramidis and the paramedian lobule: congruence of climbing fiber cortical zones and the pattern of zebrin banding within the rat cerebellum. J. Neurosci. 23, 4645–4656.
Wang, V.Y., Rose, M.F., Zoghbi, H.Y., 2005. Math1 expression redefines the rhombic lip derivatives and reveals novel lineages within the brainstem and cerebellum. Neuron 48, 31–43.
Westerfield, M., 1995. The Zebrafish Book. The University of Oregon Press.

Wilson, L.J., Wingate, R.J., 2006. Temporal identity transition in the avian cerebellar rhombic lip. Dev. Biol. 297, 508–521.
Wingate, R., 2005. Math-Map(ic)s. Neuron 48, 1–4.
Wullimann, M.F., Northcutt, R.G., 1988. Connections of the corpus cerebelli in the green sunfish and the common goldfish: a comparison of perciform and cypriniform teleosts. Brain Behav. Evol. 32, 293–316.
Wullimann, M.F., Northcutt, R.G., 1989. Afferent connections of the valvula cerebelli in two teleosts, the common goldfish and the green sunfish. J. Comp. Neurol. 289, 554–567.
Wullimann, M.F., Rupp, B., Reichert, H., 1996. Neuroanatomy of the Zebrafish Brain: A Topological Atlas. Birkhäuser Verlag, Basel.
Yamada, M., Terao, M., Terashima, T., Fujiyama, T., Kawaguchi, Y., Nabeshima, Y., Hoshino, M., 2007. Origin of climbing fiber neurons and their developmental dependence on Ptf1a. J. Neurosci. 27, 10924–10934.
Zecchin, E., Mavropoulos, A., Devos, N., Filippi, A., Tiso, N., Meyer, D., Peers, B., Bortolussi, M., Argenton, F., 2004. Evolutionary conserved role of ptf1a in the specification of exocrine pancreatic fates. Dev. Biol. 268, 174–184.
Zhou, Q., Wang, S., Anderson, D.J., 2000. Identification of a novel family of oligodendrocyte lineage-specific basic helix–loop–helix transcription factors. Neuron 25, 331–3343.
Zupanc, G.K., Hinsch, K., Gage, F.H., 2005. Proliferation, migration, neuronal differentiation, and long-term survival of new cells in the adult zebrafish brain. J. Comp. Neurol. 488, 290–319.